

MOL#44396

Erlotinib Induces Mitochondrial-Mediated Apoptosis in Human H3255 Non-Small Cell Lung Cancer Cells with EGFR^{L858R} Mutation through Mitochondrial Oxidative Phosphorylation-Dependent Activation of BAX and BAK

Yi-He Ling, Ruoping Lin, and Roman Perez-Soler

Division of Medical Oncology, Albert Einstein College of Medicine, Bronx, New York 10461,
Albert Einstein College of Medicine, Bronx, New York 10461

MOL#44396

Running Title: Apoptosis induced by EGFR TKI, erlotinib

To whom correspondence should be addressed: Dr. Roman Perez-Soler, Department of Oncology, Montefiore Medical Center, 111 East 210th Street, Hofheimer 100, Bronx, New York 10467, Phone: 718-920-4001; Fax: 718-798-7474. Email: rperezso@montefiore.org

Text pages: 28

Figures: 10

References: 42

Abstract: 260 words

Introduction: 908 words

Discussion: 1321 words

Abbreviations: BMH, 1,6-bismaleimido-hexane; EGFR TKI, epidermal growth factor receptor tyrosine kinase inhibitor; DAPI, 4,6-diamidino-2-phenylindole; DMSO, dimethyl sulfoxide; FACS, fluorescence-activated cell sorter; PAGE, polyacrylamide gel electrophoresis; PMSF, phenylmethylsulfonyl fluoride; siRNA, small interfering RNA; TBST, Tris-buffered saline with Tween 20; Z-VAD-fmk, benzyloxycarbonyl-VAD-fluoromethyl ketone.

MOL#44396

ABSTRACT

EGFR TKI erlotinib shows potent anti-tumor activity in some NSCLC cell lines and is approved by FDA as second/third line treatment for NSCLC. However, the molecular mechanisms by which erlotinib induces apoptosis remain to be elucidated. Here we investigated the effect of erlotinib on apoptotic signal pathways in H3255 cells with EGFR^{L858R} mutation. Erlotinib induces apoptosis associated with the activation of caspases in a dose- and time-dependent manner. Erlotinib did not alter the expression of apoptotic receptors FAS and TRAIL, although it induced caspase-8 activation and BID cleavage. Additionally, cell death caused by erlotinib was not prevented by co-incubation with FAS and TRAIL antagonists, ZB-4 mAb and TRAIL/Fc recombinant, suggesting that erlotinib-induced apoptosis is not associated with receptor-mediated pathways. Erlotinib induces loss of mitochondrial membrane potential ($\Delta\psi_m$), and release of cytochrome c and Smac/DIABLO from mitochondria. Furthermore, erlotinib causes BAX translocation to mitochondria, BAX and BAK conformational changes and oligomerization. Erlotinib did not induce ROS generation, and co-treatment with antioxidants did not alter erlotinib-induced activation of BAX and BAK and apoptosis. However, co-treatment with inhibitors of mitochondrial oxidative phosphorylation significantly blocked erlotinib-induced activation of BAX and BAK and cell death. Z-VAD-fmk had no effect on erlotinib-induced BAX and BAK activation, but effectively prevented apoptosis. Over-expression of BCL-2 caused a significant attenuation of erlotinib-induced cell death, but not effect on BAX and BAK activation. Down-regulation of BAX and BAK gene expression with siRNA led to an effective reduction of erlotinib-induced apoptosis. Our data indicate that activation of BAX and BAK plays a critical role in the initiation of erlotinib-induced apoptotic cascades.

MOL#44396

INTRODUCTION

The epidermal growth factor receptor (EGFR) is involved in the regulation of cell proliferation, survival, differentiation, and motility (Yarden and Ullrich, 1988; Yarden and Sliwkowski, 2001). Overexpression of the EGFR family members is found in several human malignancies—including cancers of the lung, head and neck, brain, bladder and breast (Salomon et al., 1995). Several compounds that directly target the EGFR signaling pathway and have significant antitumor activity have been developed in the last few years (Noonberg and Benz, 2000). Erlotinib (TarcevaTM, OSI-774) is an orally bioavailable quinazoline derivative (Moyer et al., 1997). Preclinical studies demonstrated that erlotinib inhibits tumor cell growth coupled with inhibition of EGFR activation. Erlotinib as a single agent has shown significant clinical activity in previously treated patients with NSCLC (Pollack et al., 1999) and has received by the FDA approval as second and third line treatment for NSCLC patients (Shepherd et al., 2005). Although erlotinib-induced antitumor activity is linked to the inhibition of EGFR and its related downstream pathways, the precise cellular and molecular mechanisms by which erlotinib induces cell death remain to be elucidated. Furthermore, several studies have clearly showed that human NSCLC cells with EGFR domain mutations are super sensitive to EGFR TK inhibitors (Paez et al., 2004; Lynch et al., 2004), and that such sensitization may be involved by activation of apoptotic pathways (Tracy et al., 2004).

Apoptosis is a highly and genetically regulated cell suicide response to facilitate the correct development and homeostasis of multicellular organisms (Green, 2001). In addition, apoptosis is an important mechanism of antitumor drug-induced cell killing and susceptibility to apoptosis of tumor cells is an important determinant of chemotherapy efficacy (Kaufmann and Earnshaw, 2000). Currently, two major apoptotic pathways have been well characterized. One is the cell death receptor-mediated (extrinsic) pathway. Upon activation of the death receptor such

MOL#44396

as FAS/CD95/Apo1 or TRAIL/Apo2L, the apoptotic cascade is triggered by recruitment of adaptor molecule FADD and procaspase-8, forming the death-inducing signaling complex (DISC). Recruitment of caspase-8 to DISC leads to downstream activation of effector caspase-3 and caspase-7 (Walczak and Krammer, 2000). Caspase-8 is involved in the activation of the mitochondrial pathway via the cleavage of the BCL-2 family member BID (Li et al., 1998). The second apoptosis signal pathway is the mitochondrial-mediated apoptotic (intrinsic) pathway, which is activated by various stimuli such as DNA damage and most types of chemotherapeutic agents (Kroemer et al., 1995). Upon activation of the intrinsic pathways, the mitochondrial integrity is disrupted as a result of changes in the mitochondrial membrane potential and release of cytochrome c, and consequently resulting in the activation of caspase-9 (Reed, 2002). Activated caspase-9 directly cleaves and activates the executioner caspase-3 and caspase-7, and the activated caspase-3 and caspase-7 lead to the cleavage of a numbers of proteins, chromatin condensation, DNA laddering and formation of apoptotic bodies. In both signal pathways, BCL-2 family proteins play a crucial role in the regulation of apoptotic events (Huang and Strasser, 2000). Over-expression of BCL-2 or BCL-xL results in prevention of apoptosis. On the other hand, over-expression of BAX and BAK leads to an increase in cell susceptibility to apoptotic signals (Karbowski et al., 2006). Apart from alteration in gene expression of BCL-2 family, current studies show that BAX and BAK proteins undergo a set of activation steps in response to apoptotic stimuli (Desagher and Martinou, 2000). Upon initiation of the apoptotic cascade, BAX translocated from cytoplasm to mitochondria, both BAX and BAK proteins change their conformation, and form homooligomers (Suzuki et al., 2000). On the outer membrane of the mitochondria, oligomerized BAX and BAK may form a channel or membrane pore, which allows the release of cytochrome c, and Smac/DIABLO (Annis et al., 2005).

Recently, several reports have demonstrated that EGFR TK inhibitors including gefitinib and erlotinib induce apoptosis in NSCLC cell lines though the activation of intrinsic pathways mediated by the induction of BH3-only BIM protein (Costa et al., 2007; Cragg et al., 2007; Deng

MOL#44396

et al., 2007; Gong et al., 2007). In addition, Kuroda et al. (2006) demonstrated that activation of BH3-only BCL-2 proteins, BIM and BAD, played the key roles in imatinib-induced cell death in Bcr/Abl+ leukemic cells. In this study, we utilized human H3255 NSCLC cells harboring an EGFR^{L858R} mutation as a model to examine the molecular mechanism of erlotinib-induced apoptosis. We found that 0.1 μ M erlotinib induces apoptosis as early as 8 h following cell exposure. We also found that erlotinib-induced apoptosis is not dependent on the FAS/CD95/Apo1- and TRAIL/Apo2L-related pathways although it caused BID cleavage and activation of caspase-8. Erlotinib-induced apoptosis was clearly mediated by activation of mitochondrial-mediated pathways, resulting in the loss of mitochondrial membrane potential ($\Delta\psi_m$), and release of cytochrome c and Smac/DIABLO from mitochondria to cytoplasm. More importantly, we found that the induction of apoptosis by erlotinib involves the activation of BAX and BAK, including their conformational changes and oligomerization. Furthermore, we found that erlotinib-induced BAX and BAK activation and apoptosis are largely dependent on mitochondrial oxidant phosphorylation, but not dependent on intracellular redox. Additionally, we tested the effects of caspase inhibitors, or over-expression of BCL-2 on BAX and BAK activation and apoptosis induced by erlotinib. Down-regulation of BAX and BAK gene expression with siRNA resulted in an effective reduction of erlotinib-induced cell death. Overall, these observations provide a more detailed understanding of the mechanisms of action of the EGFR TK inhibitor erlotinib and should constitute more rational basis for its therapeutic use either alone or in combination with other chemotherapeutic agents.

MATERIALS AND METHODS

Antibodies and Chemicals. Erlotinib was obtained from OSI pharmaceuticals (Melville, NY), dissolved in DMSO at a stock concentration of 10 mM, and diluted to the indicated concentration with RPMI-1640 medium. The polyclonal antibodies of caspase-3, caspase-8,

MOL#44396

caspace-9, FADD, BID, and BAX were purchased from Cell Signaling (Beverly, MA), the antibodies of FAS, TRIAL, and cytochrome c were purchased from Santa Cruz Bio (Santa Cruz, CA); monoclonal antibody of BCL-2, BAX and polyclonal antibody of Smac/DIABLO were purchased from Calbiochem (La Jolla, CA). Rotenone, antimycin A, oligomycin, and Z-VAD-fmk were purchased from Biomol (Plymouth, PA). Other chemicals were purchased from Sigma-Aldrich Co. (St. Louis, MO).

Cell Lines. The human H3255 NSCLC cell line carrying an L858R EGFR mutation was a generous gift from Dr. Janne (Harvard Medical School, Boston, MA), and H322 cell line with wild type of EGFR was purchased from American Type Culture Collection (Manassas, VA). Cells were maintained in 75 cm² flask in RPMI-1640 medium supplement with 10% fetal bovine serum, 100 units/ml penicillin, and 100 µg/ml streptomycin at 37°C in a humidified atmosphere with 5% CO₂.

Assay of Apoptosis and Cell Death. H3255 cells were treated with 0.1 µM erlotinib for the indicated times. Following treatment, cells were fixed with 4% paraformaldehyde in PBS for 5 min, and stained with DAPI (0.5 µg/ml) in PBS for 15 min. Apoptotic cells (50 cells from three different fields) were counted with a Nikon E400 fluorescence microscopy. For sub-G0/G1 assays, cells were fixed with 75% cold ethanol at 4°C overnight, and then incubated at room temperature for 3 h with 1 µg/ml propidium iodide and 5 µg/ml RNase I (Roche Molecular Biochemicals, Indianapolis, IN). The number of apoptotic cells (sub-G0/G1) was measured by FACScan flow cytometry (BD Biosciences, San Jose, CA). For annexin V assay, cells treated with erlotinib were double-stained with FITC-conjugated annexin V and propidium iodide using a kit according to manufacturer's instruction (Calbiochem). The percentage of annexin V positive cells was assessed by FACScan flow cytometry. For cell death assays, cells were treated with erlotinib for the indicated times, and cell survivals were determined by trypan blue exclusion.

MOL#44396

Assay of Caspase Activity. H3255 cells were treated with 0.1 μM erlorinib for the indicated times. Following treatment, cells were extracted with extraction buffer contained 20 mM HEPES, pH 7.2, 100 mM NaCl, 0.1% CHAPS, 10 mM DTT, 1 mM EDTA, 10% sucrose, 1 mM PMSF, 10 $\mu\text{g/ml}$ leupeptin, and 10 $\mu\text{g/ml}$ aprotinin at 4°C for 15 min. The soluble extracts were collected by centrifugation at 14,000g at 4°C for 15 min, and stored at -80°C until assayed. Ten μl of cell extracts (10-30 μg of protein) were added into total 100 μl reaction mixture containing 12 μM Ac-DEVD-pNA, Ac-IETD-pNA, or Ac-LEHD-pNA (Biomol) as the substrates for caspase-3, caspase-8, and caspase-9, respectively in a 96-well plate. After incubation at room temperature for 120 min, the amount of p-nitroanilline-derived substrate cleavage by caspases was determined in a microplate reader (Molecular Devices, Sunnyvale, CA) at 405 nm.

Measurement of Mitochondrial Membrane Potential ($\Delta\psi\text{m}$) and ROS. Cells were plated in a 6-well plate and treated with 0.1 μM or the same volume of medium containing 0.01% DMSO as a control for the indicated time periods. Following treatment, cells were incubated with 5 μM JC-1 (Invitrogen, Carlsbad, CA) at 37°C for 15 min for determination of $\Delta\psi\text{m}$, or with 10 μM DCF-DA (2',7',7'-dichlorofluorescein diacetate, Invitrogen) at 37°C for 30 min for measurement of ROS. After incubation, cells were harvested and washed with PBS for three times. Mitochondrial membrane potential ($\Delta\psi\text{m}$) and ROS generation were analyzed by FACScan flow cytometry.

Cellular Fractionation. For assay of release of cytochrome c, Samc/DIABLO, and BAX translocation, cells were fractionated into cytosolic and mitochondrial fractions as previously described (Ling et al, 2003). In brief, cells were incubated in buffer containing 20 mM HEPES-KOH, pH 7.2, 10 mM KCl, 1.5 mM MgCl_2 , 1 mM EDTA, 0.1 mM PMSF, 10 $\mu\text{g/ml}$ of leupeptin, 10 $\mu\text{g/ml}$ of aprotinin, at 4°C for 10 min, and then cells were homogenized with a Dounce homogenizer for 20 strokes. Following addition of buffer containing 210 mM mannitol, 70 mM sucrose, 5 mM EGTA, and 5 mM Tris-HCl, pH 7.5, the homogenates were centrifuged at 1,000g

MOL#44396

for 10 min at 4°C. The supernatants were further centrifuged at 15,000g for 30 min at 4°C, and collected as the cytosolic fraction. The pellet was further dissolved with lysis buffer containing with 1% SDS as the mitochondrial fraction.

Immunoblot Analysis. Cells were scraped from culture dish, washed twice with cold PBS solution, and then suspended in lysis buffer containing 50 mM Tris-HCl, pH 7.5, 150 mM NaCl, 1 mM EDTA, 1 mM EGTA, 1 mM NaF, 1 mM PMFS, 1mM DTT, 20 µg/ml leupeptin, 20 µg/ml aprotinin, 1% Triton X-100, and 1% SDS at 0-4°C for 15 min. After centrifugation at 15,000g for 10 min at 0°C, the supernatants were collected, and the protein amount of cell lysate was measured with a Bio-Rad protein DC assay kit (Bio-Rad, Hercules, CA). An equal amount of cell lysate (30 µg of protein) was subject to 12% or 15% SDS PAGE. Following electrophoresis, protein blots were transferred to a nitrocellulose membrane. The membrane was blocked with 5% nonfat milk in TBST solution, and incubated at 4°C overnight with the corresponding primary antibodies in the blocking solution. After washing three times with TBST solution, the membrane was incubated at room temperature for 1 h with horseradish peroxidase-conjugated secondary antibody diluted with TBST solution (1:1,000). The detected protein signals were visualized by an enhancement chemiluminescence reaction system as recommended by the manufacturer (Amersham, Arlington Heights, IL).

Flow Cytometric Analysis of BAX and BAK Activation. H3255 cells were treated with 0.1 µM erlotinib or the same volume of medium as control for the indicated times. Following treatment, cells were fixed with 0.25% paraformaldehyde in PBS at room temperature for 5 min, washed three times with PBS, and then incubated with 6A7 monoclonal anti-BAX antibody (BD Biosciences), or with AM03 monoclonal anti-BAK (Ab1) antibody (Calbiochem) in PBS containing 0.05% digitonin for 30 min. After washing three times with PBS, cells were incubated with FITC-conjugated anti-mouse antibody for 30 min in dark room, and then cells (10,000/sample) were analyzed by FACS flow cytometry. For validation of conformational

MOL#44396

change in BAX and BAK, we performed the cell lysates with Zwitterionic detergent Chaps lysis buffer (10 mM HEPES, pH 7.4, 150 mM NaCl, 1% Chaps), and immunoprecipitation with monoclonal anti-BAX (6A7) antibody and anti-BAK (Ab1) antibody according to the methods of Yamaguchi and Wang (2002). The amounts of activated BAX and BAK were detected by immunoblot using polyclonal anti-BAX and BAK antibodies.

In vitro Cross-linking for Detection of BAX and BAK Oligomers. In vitro cross-linking for detection of BAX and BAK oligomers was performed according to the methods of Sundararajan et al. (2001). In brief, cells (1×10^6 cells) were incubated in 0.5 ml of cross-linking buffer (210 mM mannitol, 70 mM sucrose, 1 mM EGTA, 5 mM HEPES, pH 7.4, 0.05% digitonin) containing 1 mM BMH (Pierce) or the same volume of DMSO as a vehicle at room temperature for 30 min. Following incubation, cells were pelleted by centrifugation at 15,000g for 15 min at 4°C, and suspended in lysis buffer (62.5 mM Tris-HCl, pH 6.8, 10% glycerol, 2% SDS). The BAX and BAK oligomers were detected by immunoblot using polyclonal anti-BAX antibody or monoclonal anti-BAK antibody, respectively.

Transient Transfection of BCL-2. Vector and human wild type BCL-2 cDNA was a gift from Dr. Xiaobo Cao (Texas A&M, College Station, TX). H3255 cells were plated in a 6-well plate, and grown at about 70% confluence. Cells were transiently transfected with 4 µg/ml of vector or BCL-2 cDNA by using Lipofectamine 2000 (Invitrogen) according to the manufacturer's instruction. Following a 4-h transfection period, cells were re-incubated in fresh medium with 10% fetal bovine serum at 37°C for 24 h. Then 0.1 µM erlotinib or the same volume of medium containing 0.01% DMSO were added to the cell culture, and incubated for an additional 24 h. Following treatment, the transfected cells were harvested and divided into two cell aliquots for the determination of BCL-2 protein expression and apoptosis as described above. For determination of the effect of BCL-2 on BAX and BAK activation, transfected cells were immunoprecipitated by anti-BAX (6A7) and anti-BAK (Ab1) antibodies, or incubated in 1mM

MOL#44396

BMH cross-linker buffer for 30 min as described above, and the active BAX and BAK were detected by immunoblot using the corresponding antibodies.

Knockdown of BAX and BAK Gene Expression with siRNA. BAX-siRNA, BAK-SiRNA, and nonspecific control of siRNA were purchased from Dharmacon (Lafayette, CO), which are SMARTpool^{MT} containing four pooled SMARTselected siRNA duplexes. Transfections of siRNA were performed according to the manufacturer's instructions. Briefly, H3255 cells were plated in a 6-well plate, and grown at about 70% confluence. Cells were transfected by using Lipofectamine 2000 (Invitrogen) with 50 pmol siRNA/10⁵ cells one day before initiating treatment with erlotinib. After 24 h of incubation, cells were harvested for the determination of BAX and BAK protein expression, and apoptosis as described above.

Statistical Analysis. Data are presented as mean \pm S.D. of the number of experiments indicated. The comparisons were made with a *t* test and the difference was considered to be statistically significant if the *p* value was <0.05.

RESULTS

Erlotinib Induces Apoptosis in H3255 Cells. Because human H3255 NSCLC cells that carry an EGFR^{L858R} mutation have shown to be very sensitive to gefitinib (Tracy et al., 2004), we selected this cell line as a model to determine the effect of erlotinib on triggering apoptotic pathways. Initially, we treated H3255 cells with 0.1 μ M erlotinib for 24 h to evaluate drug-induced apoptosis. As shown in Fig. 1A, erlotinib induces H3255 cell death with the characteristic apoptotic features, including cell detachment, shrinkage, and generation of apoptotic bodies as observed with a phase-contrast microscope, as well as the chromatin condensation and fragmentation in nucleus detected by cell staining with DAPI solution. Moreover, flow cytometric analysis revealed that erlotinib treatment led to an increase in apoptotic nuclei with a subdiploid DNA content (sub-G0/G1) (Fig. 1B), as well as an increase in the FITC-labeled annexin V positive staining cells with exposure of phosphatidylserine on the

MOL#44396

outside of the plasma membrane (Fig. 1C). The kinetic studies showed that induction of apoptosis in H3255 cells by erlotinib occurred in a concentration- and time-dependent manner. It could be detected at a concentration as low as 0.05 μM for 24 h and as early as 8 h after exposure to 0.1 μM erlotinib (Fig. 1D and E). We next explored whether erlotinib-induced apoptosis was associated with activation of caspases. Following treatment with 0.1 μM erlotinib for the indicated times, cells were harvested, and divided into two aliquots. One was used for determination of the generation of the active form of cleaved caspases by immunoblots. The other was used for determination of caspase activities measured by the colorimetric assay as described in Materials and Methods. The immunoblot analysis revealed that 0.1 μM erlotinib treatment resulted in the appearance of the active forms of cleaved caspase-8 (43 and 18 kDa) and caspase-9 (37 and 35 kDa) as early as 4 h after drug exposure, and the active forms of cleaved caspase-3 (26, 19, and 17 kDa) after 8 h of drug exposure (Fig. 1F). Consistently, quantitative determinations of caspase activities by colorimetric assays showed that activities of caspase-8 and caspase-9 were markedly increased by about 2.8- and 2.4-fold at 4 h of erlotinib treatment, respectively; whereas caspase-3 activity was increased by about 2.9-fold after 8 h of drug treatment (Fig. 1G). These results indicate that erlotinib triggers the initiator caspase-8, and caspase-9 initially and subsequently activates the executioner caspase-3.

Effect of Erlotinib on Extrinsic Apoptotic Pathways. Because erlotinib treatment caused a remarkable activation caspase 8, which is an initiator of caspase in the extrinsic apoptosis pathways (Walczak and Krammer, 2000), we sought to determine whether the death receptor apoptotic signals were involved in erlotinib-induced apoptosis. Results as shown in Fig. 2A indicate that erlotinib at 0.1 μM caused a time-dependent caspase-8 induced cleavage of BH3-only BID protein and the formation of its truncated form (t-BID), which could translocate to the mitochondria to enhance the mitochondrial-mediated apoptosis pathways (Li et al., 1998). Under the same experimental conditions, erlotinib did not markedly affect the expression of the death

MOL#44396

receptors FAS and TRAIL as well as FAS adaptor protein FADD over time (Fig. 2B). To further explore whether erlotinib-induced apoptosis is associated with the death receptor pathways, we treated H3255 cells with 0.1 μ M erlotinib alone, or plus 2 μ g/ml of FAS-antagonistic mAb (ZB-4, Upstate, Charlottesville, VA), or 2 μ g/ml of TRAIL antagonistic TRAIL/Fc recombinant (Apotech, San Diego, CA) for 24 h. Neither ZB-4 mAb nor TRAIL/Fc recombinant protected against erlotinib-induced cell death, whereas co-treatment with ZB-4 mAb resulted in a significant reduction of FAS-induced cell death ($p < 0.01$), and co-treatment with TRAIL/Fc attenuated TRAIL-induced cell death ($p < 0.05$) (Fig. 2C and D). These results suggest that erlotinib-induced apoptosis may not be mediated with FAS/CD95/Apo1 and/or TRAIL/Apo2L apoptotic pathways, although erlotinib induces caspase-8 activation and generation of t-BID.

Erlotinib Induces Mitochondrial Dysfunction. Next we examined whether erlotinib-induced apoptosis was mediated with the mitochondrial pathways. First we treated H3255 cells with 0.1 μ M erlotinib for the indicated time and then determined its effect on the mitochondrial membrane potential ($\Delta\psi_m$) using the cationic dye JC-1. As shown in Fig 3A, the typical fluorescence histograms show that disruption of $\Delta\psi_m$ determined by the ratio of JC-1 aggregates to monomers was observed in cells treated with 0.1 μ M after 8 and 24 h, as compared with control cells. Quantitative analysis of $\Delta\psi_m$ loss measured by JC-1 aggregates at FL-2 indicated that ~ 30% of loss of $\Delta\psi_m$ was observed after 8 h of erlotinib treatment, increasing over time compared at each time point with control cells (Fig. 3B). Second, we evaluated the effect of erlotinib on cytochrome c release from mitochondria to the cytoplasm by immunoblot analysis after cell fractionation. As shown in Fig.3 C, the signal of cytochrome c was barely detectable in cytosol at times 0-4 h and clearly detected at 8 h, reached the maximal level thereafter. Under the same experimental conditions, we also detected the release of Smac/DIABLO, another apoptotic regulator, from mitochondria to cytosol with a pattern similar to that of cytochrome c release.

MOL#44396

Erlotinib Induces BAX Translocation to the Mitochondria and Conformational Changes of BAX and BAK. Previous reports have demonstrated that BAX translocation to the mitochondria and alteration in protein conformation of BAX and BAK are necessary steps in cells undergoing apoptosis (Desagher et al., 2000; Stankiewicz et al., 2005). We thus examined whether erlotinib-induced apoptosis is associated with the activation of BAX and BAK. We investigated BAX localization in the cytosol and mitochondria after cell fractionation by immunoblots in H3255 cells following exposure to 0.1 μ M erlotinib for the indicated times. As shown in Fig. 4A, BAX levels were high in the cytosol at 0-4 h of incubation, and then declined at 8-24 h. In contrast, BAX levels in the mitochondrial fraction were low at 0-4 h post drug exposure, and increased thereafter, indicating that erlotinib treatment led to BAX translocation to the mitochondria. In addition, we found that erlotinib did not markedly alter the subcellular localization of BAK over time, remaining in the mitochondria all along (data not shown). Next, we analyzed the activity-related conformational changes in BAX and BAK by flow cytometric analysis using immunostaining with special anti-BAX (6A7) and BAK (AM03, Ab1) antibodies, which recognize the N-terminal epitopes of the active conformation of BAX and BAK (Panaretakis et al., 2002). The typical fluorescence histograms shown in Fig. 4B and C (top panels), demonstrate that exposure to 0.1 μ M erlotinib induces a shift to the right of the BAX and BAK fluorescence curves as compared with control, indicating that erlotinib leads to BAX and BAK activated conformational changes. The quantitative analysis presented in Fig. 4B and C (bottom panels), indicates that the increased BAX and BAK activities occurred as early as 4 h after erlotinib exposure and gradually increased with time. To further validate these observations, we utilized the zwitterionic detergent Chaps, which has been proven to retain the BAX and BAK at native conformation (Yamaguchi and Wang, 2002), to prepare cell lysate and then to immunoprecipitate BAX and BAK proteins with anti-BAX 6A7 and anti-BAK Ab-1 antibodies. As shown in Fig. 4D, the signal of active BAX was barely detectable at time 0, was first detected

MOL#44396

at 4 h of erlotinib exposure, and remained elevated thereafter; whereas the level of active BAK was low at time 0 and gradually increased with time (Fig. 4E). However, the bands of BAX and BAK in the cell lysates extracted with nonionic detergent NP-40 remained constant at all time points. These data indicated that erlotinib induces BAX translocation to mitochondria, and BAX and BAK conformational changes.

Erlotinib Induces BAX and BAK Oligomerization. Recent studies have demonstrated that oligomerizations of BAX and BAK play a critical role in triggering mitochondrial-mediated apoptosis (Suzuki et al., 2000; Antignani and Youle, 2006). We explored whether oligomerizations of BAX and BAK are involved in erlotinib-induced apoptosis. To address this issue, H3255 cells were exposed to varying concentrations of erlotinib for 24 h or to 0.1 μM erlotinib for the indicated times. After exposure, cells were treated with membrane-permeable protein cross-linker BMH, and then the oligomers of BAX and BAK were detected by immunoblots using the corresponding antibodies. As shown in Fig. 5A and B, erlotinib strongly induces the formation of BAX and BAK homodimer (42 kDa and 52 kDa), and homotrimer (63 kDa and 78 kDa) with two bands of slower mobility than that of their monomer (21 kDa, and 26 kDa) in a concentration- and time-dependent manner. For example, the signals of BAX dimer and trimer were barely detectable at 0 μM and time 0, but clearly detectable in cells following exposure to erlotinib at a concentration as low as 0.01 μM for 24 h or to 0.1 μM as early as at 2 h. Similarly, erlotinib-induced BAK dimer and trimer occurred at concentration as low as 0.01 μM and as early as at 2 h of drug exposure, although the BAK dimer was also detected in a concentration at 0 μM and time 0.

Erlotinib-induced BAX and BAK Activation is Independent of ROS Generation. A number of reports have demonstrated that the generation of reactive oxygen species (ROS) or modulation of intracellular redox plays a critical role in the regulation of activation of BAX and BAK (Zheng et al., 2005). We sought to investigate whether erlotinib-induced apoptosis and

MOL#44396

activation of BAX and BAK could be tied to ROS generation. We first examined the intracellular ROS level by flow cytometric analysis after incubation with DCF-DA in cells treated with 0.1 μM erlotinib for 6 h. As shown in Fig. 6 A, erlotinib treatment not only did not induce but actually suppressed slightly the generation of ROS as shown by the left shifting of the ROS fluorescence curve, whereas H_2O_2 as a positive control led to ROS generation as showing by the right shift of the ROS fluorescence curve, as compared with control cells (B). In parallel, we tested the effects of the antioxidants *N*-acetylcysteine (NAC), tiron (4,5-dihydroxy-1,3-benzendisulfonic acid disodium salt), and GSH (reduced glutathione) on erlotinib-induced activation of BAX and BAK and apoptosis, and found that all tested antioxidants failed to alter drug-induced apoptotic cell death (Fig. 6 C), and to affect erlotinib-induced BAX and BAK conformational changes and oligomerization (Fig. 6D and E). These results suggest that erlotinib-induced cell death is not dependent on ROS-mediated pathways.

Effects of Inhibitors of Mitochondrial Oxidative Phosphorylation on Erlotinib-Induced Activation of BAX and BAK and Apoptosis. Recent investigations have demonstrated that the activation of BAX and BAK may be controlled by either mitochondrial oxidative phosphorylation and/or by mitochondrial membrane permeabilization (Tomiya et al., 2006). We thus tested the role of mitochondrial oxidative phosphorylation in the regulation of erlotinib-induced activation of BAX and BAK and cell death. We first determined the effects of rotenone (1 μM), antimycin A (5 μM), two inhibitors of mitochondrial electron transport chain complexes I and II (Okun et al., 1999), and oligomycin (3 μM), an inhibitor of mitochondrial ATPase (F_1F_0) (Linnett and Beechey, 1979), on the activation of BAX and BAK as measured by conformational change and oligomerization, and on the mitochondrial dysfunction as monitored by cytochrome c release in H3255 cells following exposure for 12 h with 0.1 μM erlotinib. We found that co-treatment with these inhibitors effectively blocked erlotinib-induced BAX and BAK activation including the reduction of the formation of active BAX and BAK, and decline in

MOL#44396

BAX and BAK oligomerization (Fig. 7A and B), and protected cytochrome c release to cytosol as compared with cells treated with erlotinib alone (Fig. 7C). Consistently, co-treatment with these inhibitors caused a significant inhibition of erlotinib-induced apoptosis as compared with cells treated with erlotinib alone ($p < 0.01$) (Fig. 7D). These data indicate that the activation of BAX and BAK by erlotinib is clearly dependent on mitochondrial oxidative phosphorylation.

Effects of Caspase Inhibitor on Erlotinib-induced Activation of BAX and BAK and Apoptosis. Since erlotinib-induced apoptosis correlates with the activation of caspases, we examined whether the activation of BAX and BAK by erlotinib could be linked to the caspase-dependent pathway. To this purpose, we co-treated H3255 cells with 0.1 μM erlotinib and 50 μM Z-VAD-fmk, a pan-caspase inhibitor for 24 h, and then examined the effect on induction of apoptosis. As shown in Fig. 8A, co-treatment with Z-VAD-fmk led to a complete prevention of erlotinib-induced apoptosis. However, co-treatment with Z-VAD-fmk had no effect on erlotinib-induced BAX and BAK conformational changes and oligomerization (Fig. 8 B and C). These results suggest that BAX and BAK activation may not be through the caspase-dependent pathway, and caspase activation is downstream of BAX and BAK activation in erlotinib-induced apoptosis.

Effect of Over-expression of BCL-2 on Erlotinib-induced BAX and BAK Activation and Apoptosis. It has been well established that BCL-2 plays a critical role in the regulation of the mitochondrial-mediated apoptotic pathway (Adams and Cory, 2001). We thus transiently transfected H3255 cells with BCL-2 cDNA, and determined the effect of over-expression of BCL-2 on erlotinib-induced the activation of BAX and BAK, and apoptosis. Immunoblot analysis revealed that endogenous BCL-2 was barely detectable in nontransfected and vector transfected cells, and BCL-2 expression was clearly detected after a 24-h BCL-2 cDNA transfection (Fig. 9A). As expected, transient transfection of BCL-2 led to a significant inhibition of erlotinib-induced cell death, i.e. ~14% of cells were apoptotic in H3255/BCL-2 cells as compared with ~27% in H3255 and H3255/Vector cells following a 24-h treatment with 0.1 μM erlotinib (Fig.

MOL#44396

9B). However, we also found that BCL-2 overexpression did not markedly alter erlotinib-induced BAK conformational change and oligomerization, and slightly reduced the formation of active form of BAX and dimer (Fig. 9C and D). These data suggest that overexpression of BCL-2 may not be involved in the regulation of BAX and BAK activation although it prevented erlotinib-induced cell death.

Effect of Down-regulation of BAX and BAK Gene Expression by siRNA on Erlotinib-induced Apoptosis in H3255 Cells. To further investigate the role of BAX and BAK expression on the regulation of cell death by erlotinib, we utilized BAX and BAK siRNA to down-regulate both proteins expression in H3255 cells, and to test the effect of down-regulation of BAX and BAK on erlotinib-induced apoptosis. As shown in Fig. 10A, immunoblot analysis demonstrated that transfection with BAX and BAK siRNA specifically down-regulated the expression of BAX and BAK protein in either control or erlotinib-treated cells as compared with nontransfected cells or cells transfected with non-specific siRNA. As expected, down-regulation of BAX or BAK protein expression by siRNA resulted in a significant attenuation of erlotinib-induced apoptosis ($p < 0.01$), whereas the non-specific siRNA transfection did not significantly alter drug-induced activation of apoptosis as compared with that of nontransfected cells (Fig. 10B). In addition, we found that the double gene silenced by transfection with both BAX and BAK siRNA caused a higher inhibitory effect on erlotinib-induced apoptosis than that observed with transfection with either BAX siRNA or BAK siRNA alone ($p < 0.05$). These findings suggest that the activation of either BAX or BAK gene may play an important role in the regulation of erlotinib-induced apoptosis.

DISCUSSION

In previous work we and others have demonstrated that erlotinib is a highly selective EGFR tyrosine kinase inhibitor with potent activity against human NSCLC cell lines in in-vitro and in-vivo studies (Moyer et al., 1997; Dai et al., 2005). We also found that erlotinib exposure

MOL#44396

caused cell growth inhibition accompanied by the cell-cycle arrest at G1/S phase in human NSCLC cell lines. The G1/S phase arrest by erlotinib was shown to be via drug-induced p27^{KIP1} up-regulation and nuclear translocation (Ling et al., 2007). In addition, recent studies have shown that EGFR gene mutations within the active loops of the tyrosine kinase domains confer very pronounced susceptibility to the EGFR TKI gefitinib in NSCLC cells (Paez et al., 2004; Lynch et al., 2004). In the present work, we used human H3255 NSCLC cells, which harbor an EGFR^{L858R} mutation, as a model to examine the sequence of events involved in the inhibition of cell proliferation and cell death induced by erlotinib. Our results show that the exposure of H3255 cells to low concentrations of erlotinib results in apoptotic cell death as verified from morphological observations and the assessment of sub-G0/G1 cells and annexin-V positive staining by FACS analysis, and is associated with the activation of caspases at the initiative and executive stages. Furthermore, we found that erlotinib did not affect the expression of the apoptotic receptors FAS and TRAIL, although it induced activation of caspase-8 and cleavage of BH3-only BID protein. Co-incubation with the FAS and TRAIL antagonists ZB-4 mAb and TRAIL/Fc recombinant did not prevent erlotinib-induced cell death, suggesting that apoptosis caused by erlotinib is not mediated by apoptotic receptor-related pathways. These results are consistent with the studies by Liu and Fan, who showed that cetuximab, an anti-human EGFR monoclonal antibody, induces cell death in DiFi colon cancer cells, but does not interact with or regulate the TRAIL or FAS related pathway although it activates caspase-8 (Liu and Fan, 2001). Our studies demonstrated that erlotinib induces the disruption of mitochondrial function with loss of $\Delta\Psi_m$, as well as release of cytochrome c and Smac/DIABLO from mitochondria to the cytosol. We also observed that erlotinib-induced apoptosis is correlated with BAX translocation from the cytosol to the mitochondria, and BAX and BAK protein conformational changes as well as both pro-apoptotic protein oligomerization. To our knowledge, the observation that activation of BAX and BAK and their oligomerization are involved in erlotinib-induced apoptosis is new. The kinetic studies showed that the activation of BAX and BAK including their conformational

MOL#44396

changes and oligomerization precede the release of cytochrome c and Smac/DIABLO and the activation of caspases and appeared to be a major contributing factor in the initiation of apoptotic signals by erlotinib. We also tested whether erlotinib-induced activation of BAX and BAK occurs in other human NSCLC cell lines. Preliminary results show that erlotinib treatment causes H322 cell death accompanied by the induction of BAX and BAK oligomerization, indicating that the activation of BAX and BAK protein is not restricted to H3255 cells (Supplementary information, Fig. S1). It has been suggested that BAX and BAK oligomerization can facilitate the formation of the megachannel in the outer mitochondrial membrane, thus allowing the release of cytochrome c. However, the precise molecular mechanisms of how the megachannel is formed and how cytochrome c is subsequently released remain unknown (Annis et al., 2005). Our results indicate that BAX and BAK oligomerization was an earlier event than BAX translocation, as well as cytochrome c release and caspase activation, suggesting that BAX and BAK oligomerization is the events triggering the apoptosis cascades. These results are consistent with the reports by Gross et al., who demonstrated that BAX oligomerization is a prerequisite for BAX translocation to the mitochondria (Gross et al., 1998). Although erlotinib induces apoptosis via the disruption of mitochondrial function and the activation of BAX and BAK, the precise mechanism by which the inhibition of EGFR and its related pathways could lead to the initiation of the apoptotic cascades remain to be further elucidated. One possible explanation for the erlotinib-induced the activation of BAX and BAK may be a direct interaction with BAX and BAK, and then inducing protein conformational changes and oligomerization. However, preliminary results show that erlotinib has no effect on protein conformation by immunostaining using active anti-BAX and BAK antibodies, and does not induce oligomerization of BAX and BAK as measured by immunoblots in the presence of protein cross-linker BMH when it is added directly into the cell-free systems such as the cytosolic or mitochondrial fractions prepared from H3255 cells (data not shown), suggesting that erlotinib does not directly interact with BAX or BAK proteins. Another possibility may be that erlotinib inhibits AKT/PKB and/or ERK/MAP kinase, and these events

MOL#44396

lead to the activation of BAX and BAK and the initiation of apoptotic cascades. We thus compared the effects of erlotinib, the inhibitors of AKT/PKB, LY-294002 and Wortmannin, and the inhibitors of ERK/MAP kinase, U-0126 and PD-98059 on the activation of BAX and BAK. We found that at pharmacological concentrations, AKT/PKB inhibitors, but not ERK/MAP kinase inhibitors cause the activation of BAX and BAK. These results suggest that erlotinib-induced activation of BAX and BAK is associated with the inhibition of AKT/PKB rather than with the inhibition of ERK/MAP kinase pathway (Supplementary information, Fig. S2). Indeed, a recent study showed that the inhibition of AKT/PKB signal pathway by either growth factor deprivation or glucose deprivation resulted in the abrogation of AKT-mediated BAX and BAK activation in mitochondria (Majewski et al., 2004).

Recently Tomiyama et al. have demonstrated that co-treatment with inhibitors of mitochondrial oxidative phosphorylation markedly prevented the oligomerization of BAX and BAK and cell death in rat-1 fibroblasts and human cancer cells subjected to apoptotic stimuli such as DNA damage, ER stress and TNF- α (Tomiyama et al., 2006). Consistently, our results also demonstrate that co-treatment with a variety of inhibitors of mitochondrial oxidative phosphorylation including rotenone, antimycin A, and oligomycin effectively blocked erlotinib-induced the formation of active BAX and BAK, and oligomerization, and cytochrome c release as well as cell death. These data indicate that BAX and BAK activation by erlotinib may be regulated by mitochondrial oxidative phosphorylation and/or with the modulation of mitochondrial membrane permeabilization. The other possibility may be that erlotinib treatment could alter the oxidative-phosphorylation metabolic pathways and metabolites such as alteration in the glycolysis for ATP generation, and/or changes in NADPH oxidase in the membrane and the mitochondrial electron transport system (Harris and Daniel, 1989).

In summary, our results demonstrate that erlotinib-induced apoptosis in H3255 cells is associated with activation of caspases at initiative and executive stages. Erlotinib-induced apoptosis is dependent on the mitochondrial-mediated pathway, but independent of extrinsic

MOL#44396

pathway. Furthermore, the activation of BAX and BAK including BAX translocation, BAX and BAK conformational changes, and oligomerization plays a crucial role in the initiation of erlotinib-induced apoptosis. In addition, the activation of BAX and BAK is dependent on the mitochondrial oxidative phosphorylation, but independent of ROS generation or redox signals. Over-expression of BCL-2 or inhibition of caspase activity by Z-VAD-fmk did not markedly affect the activation of BAX and BAK, but inhibited erlotinib-induced apoptosis. Moreover, down-regulation of BAX and BAK protein expression by siRNA led to the attenuation of erlotinib-induced apoptosis. In addition, recent investigation by Gong et al. indicated that erlotinib induced apoptosis through the alteration in the subcellular localization of BAX from nuclei to cytoplasm in PC-9 and H3255 cells (Gong et al., 2007). All findings suggest that the activation of pro-apoptotic BCL-2 proteins including BAX, BAK and BIM is essential for the triggering of EGFR TKI-induced intrinsic apoptotic pathway. Overall, the characterization of the molecular sequences of events leading to erlotinib-induced apoptosis has yielded important information toward understanding the mechanisms of action of EGFR TKIs in lung cancer cells. These findings provide a better elucidation of the mechanisms involved in erlotinib-induced apoptosis and should help optimizing the use of this compound in the clinic in combination with other agents to improve its efficacy.

MOL#44396

REFERENCES

- Adams JM, and Cory S (2001) Life-or-death decision by the Bcl-2 protein family. *Trend Biochem Sci* 26:61-66.
- Annis MG, Soucie EL, Dlugosz OJ, Cruz-Aguado JA, Penn LZ, Leber B, and Andrews W (2005) Bax form multispansing monomers that oligomerize to permeabilize membranes during apoptosis. *EMBO J* 24:2096-2103.
- Antignani A, and Youle RJ (2006) How do Bax and Bak lead to permeabilization of the outer mitochondrial membrane? *Curr Opin Cell Biol* 18:685-689.
- Costa DB, Halmos B, Kumar A, Schumer ST, Huberman MS, Boggon TJ, Tenen DG, and Kobayashi S (2007) BIM mediates EGFR tyrosine kinase inhibitor-induced apoptosis in lung cancer with oncogenic EGFR mutations. *PLoS Med* 4:e315.
- Cragg MS, Kuroda J, Puthalakath H, Huang DCS, and Strasser A (2007) Gefitinib-induced killing of NSCLC cell lines expressing mutant EGFR requires BIM and can be enhanced by BH3 mimetics. *PLoS Med* 4:e316.
- Dai Q, Ling YH, Lia M, Zou Y, Kroog G, Iwata KK, and Perez-Soler R (2005) Enhanced sensitivity to the HER1/epidermal growth factor receptor tyrosine kinase inhibitor erlotinib hydrochloride in chemotherapy-resistant tumor cell lines. *Clin Cancer Res* 11:1572-1578.
- Deng J, Shimamura T, Perera S, Carlson NE, Cai D, Shapiro G, Wong K-K, and Letai A (2007) Proapoptotic BH3-only bcl-2 family protein BIM connects death signaling from epidermal growth factor receptor inhibition to the mitochondrion. *Cancer Res* 67:11867-11875.
- Desagher S, and Martinou JC (2000) Mitochondria as the central control point of apoptosis. *Trends Cell Biol* 10:369-377.
- Gong Y, Somwar R, Politi K, Blak M, Chmielecki J, Jiang X, and Pao W (2007) Induction of BIM is essential for apoptosis triggered by EGFR kinase inhibitors in mutant EGFR-dependent lung adenocarcinomas. *PLoS Med* 4:e294.
- Green DR (2001) Apoptotic pathways: paper wraps stone blunts scissors. *Cell* 102:1-4.
- Gross A, Jennifer J, Wei M C, and Korsmeyer SJ (1998) Enforced dimerization on Bax results in its translocation, mitochondrial dysfunction and apoptosis. *EMBO J* 12:3878-3885.
- Harris RC, and Daniel TO (1989) Epidermal growth factor binding, stimulation of phosphorylation, and gluconeogenesis in rat proximal tubule. *J Cell Physiol* 139: 383-391.
- Huang DCS, and Strasser A (2000) BH3-only proteins-essential initiators of apoptotic cell death. *Cell* 103:839-842.
- Karbowski M, Norris KL, Cleland MM, Jeong S-Y, and Youle RJ (2006) Role of Bax and Bak in mitochondrial morphogenesis. *Nature* 443:658-662.
- Kaufmann SH, and Earnshaw WC (2000) Induction of apoptosis by cancer chemotherapy. *Exp Cell Res* 256:42-49.
- Kroemer G, Petit P, Zamzami N, Vayssiere JL, and Mignotte B (1995) The biochemistry of programmed cell death. *FASEB J* 9:1277-1278.
- Kuroda J, Puthalath H, Cragg MS, et al. (2006) Bim and Bad mediate imatinib-induced killing of Bcr/Abl+ leukic cells, and resistance due to their loss is overcome by a BH3 mimetic. *Proc Natl Acad Sci USA* 103:14907-14912.
- Li H, Zhu H, Xu CJ, and Yuan J (1998) Cleavage of BID by caspase 8 mediated the mitochondrial damage in the Fas pathway of apoptosis. *Cell* 98:481-490.
- Ling YH, Liebes L, Zou Y, and Perez-Soler R (2003) Reactive oxygen species generation and mitochondrial dysfunction in the apoptotic response to bortezomib, a novel proteasome inhibitor, in human H460 non-small cell lung cancer cells. *J Biol Chem* 278:33714-33723.

MOL#44396

- Ling YH, Li T, Yuan Z, Haigentz M, Weber TK, and Perez-Soler R (2007) Erlotinib, an effective kinase inhibitor, induces p27^{KIP1} up-regulation and nuclear translocation in association with cell growth inhibition and G1/S phase arrest in human non-small-cell lung cancer cell lines. *Mol Pharmacol* **72**:248-258.
- Linnett PE, and Beechey (1979) Inhibitors of the ATP synthetase systems *Methods Enzymol* **55**:472-518.
- Liu B, and Fan Z (2001) The monoclonal antibody 225 activates caspase-8 and induces apoptosis through a tumor necrosis factor receptor family-independent pathway. *Oncogene* **20**:3726-3734.
- Lynch T, Bell DW, Sordella R, et al. (2004) Activating mutations in the epidermal growth factor receptor underlying responsiveness of non-small-cell lung cancer to gefitinib. *New Eng J Med* **350**:2129-2139.
- Majewski N, Nogueira V, Robey RB, and Hay N (2004) Akt inhibits apoptosis downstream of BID cleavage via a glucose-dependent mechanism involving mitochondrial hexokinases. *Mol Cell Biol* **24**:730-740.
- Moyer JD, Barbacci EG, Iwata K, Arnold L, Boman B, Cunningham A, DiOrio C, Doty J, Morin MJ, Moyer MP et al. (1997) Induction of apoptosis and cell cycle arrest by OSI-774, an inhibitor of epidermal growth factor tyrosine kinase. *Cancer Res* **57**:4838-4848.
- Noonberg SB, and Benz CC (2000) Tyrosine kinase inhibitions targeted to the epidermal growth factor receptor subfamily: role as anticancer agents. *Drug* **59**:753-756.
- Okun JG, Lummen P, and Brandt U (1999) Three classes of inhibitors share a common binding domain in mitochondrial complex I (NADH:ubiquinone oxidoreductase. *J Biol Chem* **274**:2625-2630.
- Paez JG, Janne PA, Lee JC, et al. (2004) EGFR mutations in lung cancer: correlation with clinical response to gefitinib therapy. *Science* **304**:1497-1500.
- Panaretakis T, Pokrovakaja K, Shoshan MC, and Grandner D (2002) Activation of Bak, Bax, and BH3-only proteins in the apoptotic response to doxorubicin. *J Biol Chem* **277**:44317-44326.
- Pollack VA, Savage DM, Baker DA, Tsaparkos KE, Sloan DE, Moyer JD, et al. (1999) Inhibition of epidermal growth factor receptor-associated tyrosine phosphorylation in human carcinoma with OSI-774: Dynamics of receptor inhibition in situ and antitumor effects in athymic mice. *J Pharmacol Exper* **291**:739-748.
- Reed JC (2002) Apoptosis-based therapies. *Nat. Rev Drug Discov* **1**:111-121.
- Salomon DS, Brandt R, Ciardiello F, and Normanno N (1995) Epidermal growth factor-related peptides and their receptor in human malignancies. *Cri. Rev Oncol Hematol* **18**:183-232.
- Shepherd FA, Rodrigues PJ, Ciuleanu T, et al. (2005) Erlotinib in previously treated non-small-cell lung cancer. *N Engl J Med* **353**:123-132.
- Stankiewicz AR, Lachapelle G, Foo CPZ, Radicioni SM, and Mosser DD (2005) Tumor necrosis factor- α induces Bax-Bak interaction and apoptosis, which is inhibited by adenovirus E1B 19K. *J Biol Chem* **280**:38729-38739.
- Sundararajan R, Cuconati A, Nelson D, and White E (2001) Tumor necrosis factor- α induces Bax-Bak interaction and apoptosis, which is inhibited by adenovirus E1B 19K. *J. Biol. Chem.* **276**:45120-45127.
- Suzuki M, Youle Rj, and Tjandra N (2000) Structure of Bax: coregulation of dimer formation and intracellular localization. *Cell* **103**:645-654.

MOL#44396

- Tomiyama A, Serizawa S, Tachibana K, Sakurada K, Samejima H., Kuchino, Y, and Kitamaka C (2006) Critical role for mitochondrial oxidative phosphorylation in the activation of tumor suppression Bax and Bak. *J Natl Cancer Inst* **98**:1462-1473.
- Tracy S, Mukohara T, Hansen M et al. (2004) Gefitinib induces apoptosis in the EGFR^{L858R} non-small-cell lung cancer cell line H3255. *Cancer Res* **64**:7241-744.
- Walczak H, and Krammer PH (2000) The CD95 (APO-1/Fas) and TRAIL (APO-2L) apoptosis system. *Exp Cell Res* **256**:58-66.
- Yamaguchi H, and Wang H-G (2002) Bcl-XL protects Bim-induced Bax conformational change and cytochrome c release independent of interacting with Bax or BinEL. *J Biol Chem* **277**:41604-41612.
- Yarden Y, and Ullrich A (1988) Growth factor receptor tyrosine kinases. *Annu Re. Biochem* **57**:443-478.
- Yarden Y, and Sliwkowski MX (2001) Untangling the ErbB signaling network. *Nat Rev Mol Cell Biol* **2**:127-137.
- Zheng Y, Yamaguchi H, Tian C, Lee MW, Tang H, Wang H-G, Chen Q (2005) Arsenic trioxide (As₂O₃) induces apoptosis through activation of bax hematopoietic cells. *Oncogene* **24**:3339-3347.

MOL#44396

FOOTNOTES

This work was supported in part by NIH grant CA84119 and CA96515, and by OSI Pharmaceuticals, Inc.

MOL#44396

LEGENDS FOR FIGURES

Fig. 1. Erlotinib induces apoptosis and activation of caspases in H3255 cells. (A), Cells were treated with 0.1 μ M erlotinib or with the same volume of medium as a control for 24 h. Following treatment, cell morphological changes were visualized by phase-contrast microscopy or the condensed and fragmented nuclei were visualized by fluorescent microscopy using DAPI staining. (B), Apoptotic cells was determined by flow cytometric analysis after cell staining with propidium iodide (PI) or (C), staining with Annexin-V/PI. (D), Cells were treated with varying concentrations of erlotinib at 37°C for 24 h or (E), with 0.1 μ M erlotinib for the indicated time. Following treatment, cells were stained with PI solution, and the apoptotic cells were determined by flow cytometric analysis. Data represent the mean \pm S.D. of three independent experiments, ** $p < 0.01$ vs. concentration at 0 μ M or time at 0. (F), Cells were treated with 0.1 μ M erlotinib for the indicated time. Following treatment, cells were harvested and divided into two aliquots. One was used for determination of generation of active form of cleaved caspase-8, -9, and -3 by immunoblots using corresponding antibodies. (G), The other of cell aliquots was used for the determination of caspase activity by measurement of the release of pNA from substrates as described in Materials and Methods. Each point represents mean \pm S.D. of three independent experiments.

Fig. 2. Effect of erlotinib on extrinsic apoptotic pathway in H3255 cells. (A), Cells were treated with 0.1 μ M erlotinib for the indicated time. Following treatment, cells were harvested, and the total BID and truncated BID (t-BID) were detected by immunoblots using anti-BID antibody. β -Actin was used as a loading control. (B), Effect of erlotinib on expression of FAS, TRAIL, and FADD proteins. Cells were treated with 0.1 μ M erlotinib for the indicated time, and the levels of FAS, TRAIL, and FADD were determined by immunoblot analysis using the corresponding antibodies. β -Actin was used as a loading control. (C), Effect of ZB4 mAb on

MOL#44396

erlotinib- and FAS-induced cell death. Cells were treated with 0.1 μ M erlotinib or with 0.5 μ g/ml FAS alone or with plus 2 μ g/ml of ZB-4 mAb for 24 h. After treatment, cell death was determined by trypan blue exclusion. (D), Effect of TRAIL/Fc recombinant on erlotinib- and TRAIL-induced cell death. Cells were treated with 0.1 μ M erlotinib or with 0.1 μ g/ml TRAIL alone or with plus 2 μ g/ml TRAIL/Fc recombinant for 24 h. After treatment, cell death was determined by trypan blue exclusion. Data represent the mean \pm S.D. of three independent experiments, **p<0.01, *p<0.05.

Fig. 3. Effect of erlotinib on mitochondrial dysfunction in H3255 cells. Cells were treated with 0.1 μ M erlotinib or with the same volume of medium as a control for the indicated time. After treatment, cells were stained with JC-1 solution at 37°C for 15 min, and the mitochondrial membrane potential ($\Delta\psi_m$) was determined by flow cytometric analysis. (A), The histograms of flow cytometric analysis of mitochondrial membrane potential in H3255 cells following treatment with 0.1 μ M erlotinib or with the same volume of medium as a control for the indicated time. (B), Quantitative analysis of $\Delta\psi_m$ as detected by JC-1 at FL-2 in H3255 cells following treatment with 0.1 μ M erlotinib for the indicated time as comparison with control. Data represent mean \pm S.D. of three independent experiments, **p<0.01 compared with control. (C), Effect of erlotinib on cytochrome c release from mitochondria to cytoplasm. H3255 cells were treated with 0.1 μ M erlotinib for the indicated time. After treatment, cytosol and mitochondrial fractions were prepared as described in Materials and Methods. The levels of cytochrome c and Smac/DIABLO in cytosol and mitochondria were detected by immunoblots using the corresponding antibodies. β -Actin and Cox VI were used as cytosol and mitochondrial sample loading control, respectively.

Fig. 4. Erlotinib induces BAX translocation to the mitochondria and BAX and BAK conformational changes. (A), H3255 cells were treated with 0.1 μ M erlotinib for the indicated

MOL#44396

time. Following treatment, cytosolic and mitochondrial fractions were prepared as described above. The levels of BAX in cytosolic and mitochondrial fraction were detected by immunoblots. (B), and (C), Effect of erlotinib on BAX and BAK protein conformational changes. Cells were treated with 0.1 μ M erlotinib for the indicated times. After treatment, cells were fixed with paraformaldehyde, and then incubated with 6A7 monoclonal anti-BAX antibody or with AM03 monoclonal anti-BAK (Ab1) antibody for 60 min. Following incubation with FITC-conjugated second antibody for 30 min, the signals of activated conformation of BAX and BAK proteins were measured by flow cytometric analysis as described in Materials and Methods. The typical histograms of BAX and BAK conformational changes in cells treated with erlotinib are presented in up panel in (B) and (C), respectively. The increased folds of activities of BAX and BAK as measurement by flow cytometric analysis are presented in the bottom of (B) and (C), respectively. Data represent the mean \pm S.D. of three independent experiments. (D), and (E), Erlotinib-induced activation of BAX and BAK protein conformation was further validated by immunoprecipitation. H3255 cells were treated with 0.1 μ M erlotinib for the indicated time. Following treatment, cells were harvested and cell pellets were divided into two aliquots. One was used for the preparation of immunoprecipitation with 6A7 anti-BAX or Ab1 anti-BAK antibodies. The other of cell aliquots was lysed with non-ionic detergent lysis buffer. The levels of BAX and BAK were detected by immunoblots using polyclonal anti-BAX and anti-BAK antibodies.

Fig. 5. Erlotinib induces oligomerization of BAX and BAK proteins in H3255 cells. Cells were treated with varying concentrations of erlotinib for 24 h, or with 0.1 μ M erlotinib for the indicated time. Following treatment, cells were harvested and incubated with 1 mM protein cross-linker BMH at room temperature for 30 min. After incubation, cells were lysed with lysis buffer, and equal amount of lysates (30 μ g of protein) was subjected to a 15% SDS-PAGE. After

MOL#44396

transferring to a membrane, the oligomers of BAX (A) and BAK (B) were detected by immunoblots using the corresponding antibodies. The nonspecific bands (22 kDa) served as the sample loading control.

Fig. 6. Effect of erlotinib on ROS generation, and effects of anti-oxidative agents on erlotinib-induced BAX and BAK activation and apoptosis in H3255 cells. (A), and (B), The histograms of erlotinib- and H₂O₂-induced ROS generation. Cells were treated with 0.1 μ M erlotinib, or with 1 mM H₂O₂ at 37°C for 6 h. Following treatment, cells were incubated with 10 μ M DCH DA at 37°C for 15 min. The intracellular ROS levels were determined by flow cytometric analysis. (C), Effects of anti-oxidative agents on erlotinib-induced apoptosis. Cells were treated with 0.1 μ M erlotinib or with 0.1 μ M erlotinib plus 5 mM NAC, 1 mM tiron, and 2.5 mM GSH, or with the same volume of medium as a control at 37°C for 24 h. After treatment, cells were stained with DAPI solution, and the percentage of apoptotic cells was determined by counting condensed and fragmented nuclei. Data represent the mean \pm S.D. of three independent experiments. (D), Effects of anti-oxidative agents on erlotinib-induced BAX and BAK conformational changes. Cells were treated with erlotinib alone or with erlotinib plus anti-oxidative agents as described above. Following treatment, the active BAX and BAK were immunoprecipitated with 6A7 anti-BAX or Ab1 anti-BAK antibodies as described above. The levels of active BAX and BAK were measured by immunoblots using the corresponding antibodies. (E), Effects of anti-oxidative agents on erlotinib-induced BAX and BAK oligomerization. Cells were treated with erlotinib alone or with plus anti-oxidative agents as described above. Following treatment, cells were harvested and incubated with 1 mM protein cross-linker BMH at 37°C for 30 min. After subjecting to a 15% SDS-PAGE, the oligomerized BAX and BAK were detected by immunoblots using the corresponding antibodies. The nonspecific bands (22 kDa) served as the sample loading control.

MOL#44396

Fig. 7. Effects of inhibitors of mitochondrial oxidative phosphorylation on erlotinib-induced apoptosis and activation of BAX and BAK in H3255 cells. (A), Cells were treated with 0.1 μ M erlotinib alone or with 0.1 μ M erlotinib plus 1 μ M rotenone, 3 μ M oligomycin, 5 μ M antimycin A, or with the same volume of medium as a control at 37°C for 24 h. Following treatment, cells were harvested and the active BAX and BAK were immunoprecipitated with 6A7 anti-BAX or Ab1 anti-BAK antibodies as described above. The levels of active BAX and BAK were measured by immunoblots using the corresponding antibodies. (B), For assay of BAX and BAK oligomerization, cells were treated with erlotinib alone or plus inhibitors as described above. After treatment, cells were harvested and incubated with 1 mM protein cross-linker BMH for 30 min. The oligomerized BAX and BAK were detected by immunoblots using the corresponding antibodies as described above. (C), Inhibitors of mitochondrial oxidative phosphorylation inhibit erlotinib-induced cytochrome c release to cytosol. Cells were treated with erlotinib alone or plus the inhibitors of mitochondrial oxidative phosphorylation as described above. After treatment, cells were harvested and the cytosolic fraction was prepared as described in Materials and Methods. The levels of cytochrome c in cytosol were detected by immunoblot analysis. β -Actin was used as a loading control. (D), Effects of inhibitors of mitochondrial oxidative phosphorylation on erlotinib-induced apoptosis. Cells were treated with erlotinib alone or plus inhibitors as described above. Following treatment, cells were stained with DAPI solution, and the percentage of apoptotic cells was determined by counting the condensed and fragmented nuclei. Data represent mean \pm S.D. of three independent experiment, ** p <0.01 vs. erlotinib alone.

Fig. 8. Effect of caspase inhibitor on erlotinib-induced apoptosis and activation of BAX and BAK in H3255 cells. (A), Cells were treated with 0.1 μ M erlotinib or 50 μ M Z-VAD-fmk alone or with the combination of both agents at 37°C for 24 h. Following treatment, cells were stained with DAPI solution and apoptotic cells were determined by counting condensed and fragmented

MOL#44396

nuclei DAPI. Data represent mean \pm S.D. of three independent experiments, ** $p < 0.01$. (B), Effect of Z-VAD-fmk on erlotinib-induced BAX and BAK conformational changes. Following treatment as described above, cells were harvested and the active BAX and BAK were immunoprecipitated with 6A7 anti-BAX or Ab1 anti-BAK antibodies as described above. The levels of active BAX and BAK were measured by immunoblots using the corresponding antibodies. (C), Effects of Z-VAD-fmk on erlotinib-induced BAX and BAK oligomerization. Following treatment as described above, cells were harvested and incubated with 1 mM protein cross-linker BMH for 30 min. The oligomerized BAX and BAK were detected by immunoblots using the corresponding antibodies. The nonspecific bands (22 kDa) served as the sample loading control.

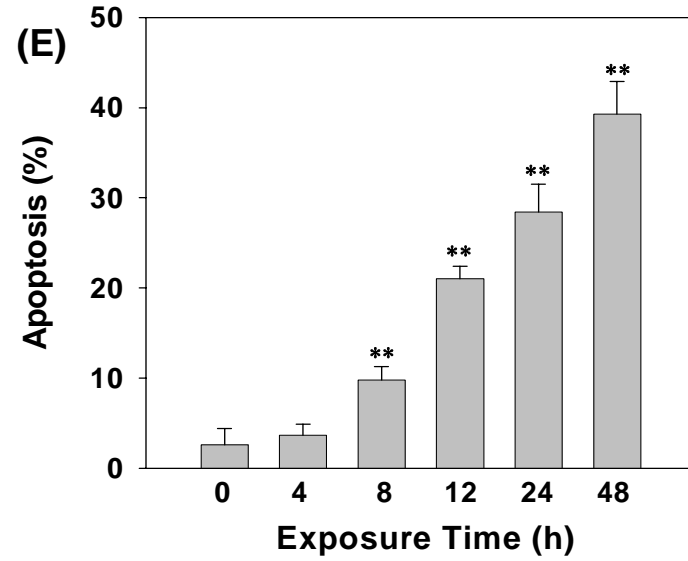
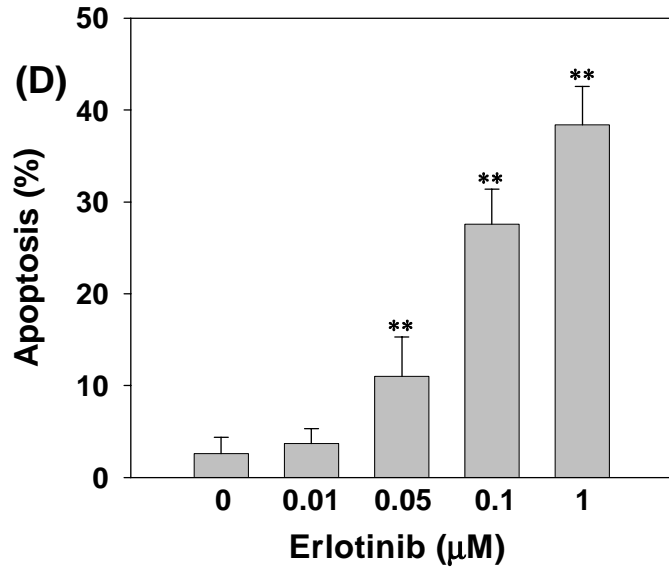
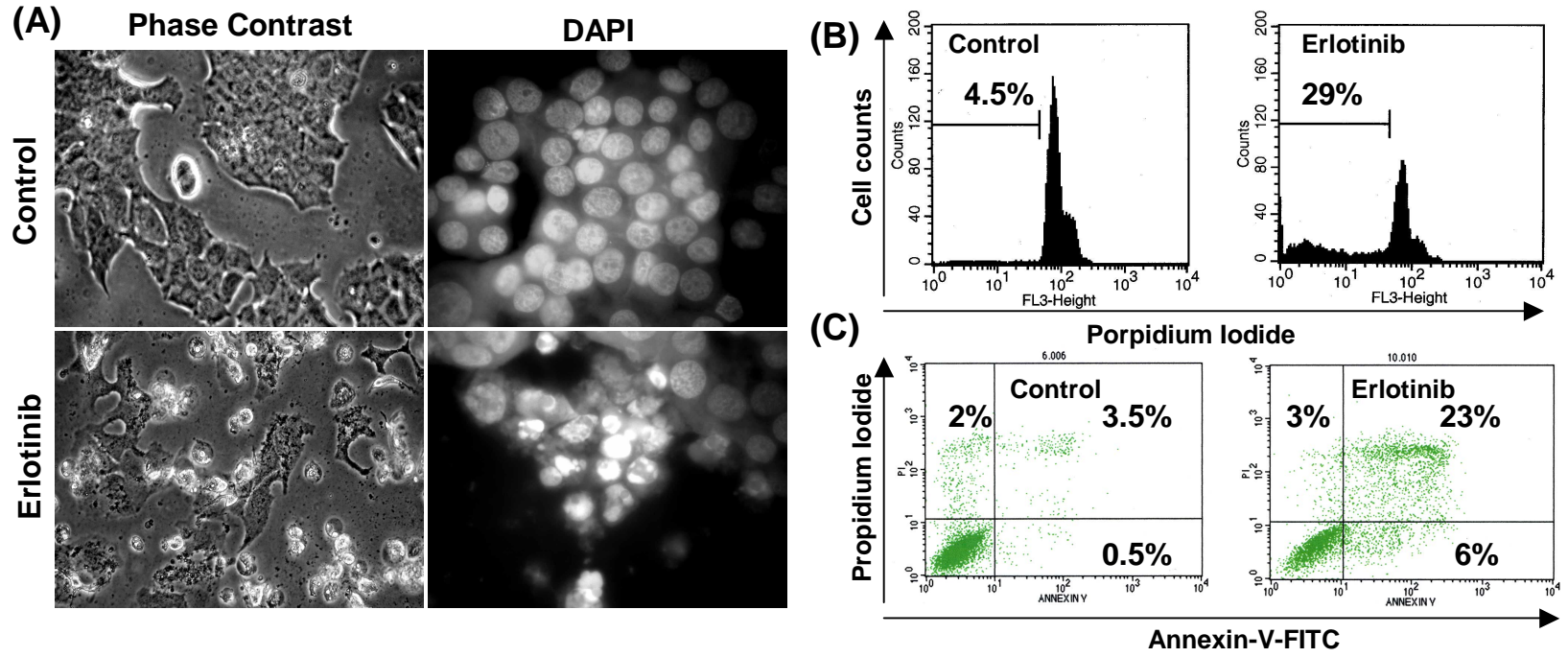
Fig. 9. Effect of transient transfection of BCL-2 cDNA on erlotinib-induced apoptosis, and activation of BAX and BAK in H3255 cells. (A), Cells were transiently transfected with 2 $\mu\text{g/ml}$ of BCL-2 cDNA or with the same amount of vector or with the same volume of medium as a control by Lipofectamine 2000 as described in Materials and Methods. Following 24 h transfection, cells were treated with 0.1 μM erlotinib, or with the same volume of medium as a control for an additional 24 h. Cells were harvested and divided into two aliquots. One was used for the determination of BCL-2 expression by immunoblots. β -Actin was used as a loading control. (B), The other of cell aliquot was used for examination of apoptotic cells after staining with DAPI as described above. Data represent mean \pm S.D. of three independent experiments, * $p < 0.05$ vs. control. (C), Effect of BCL-2 c-DNA transfection on erlotinib-induced BAX and BAK conformational changes. After BCL-2 transfection, cells were treated 0.1 μM erlotinib as described above. Following treatment, cells were harvested and the active BAX and BAK were immunoprecipitated with 6A7 anti-BAX and Ab1 anti-BAK antibodies as described above. The levels of active BAX and BAK were detected by immunoblots using corresponding antibodies.

MOL#44396

(D), Effect of BCL-2 cDNA transfection on erlotinib-induced BAX and BAK oligomerization. Cells were transiently transfected with BCL-2 cDNA and treated with erlotinib as described above. Following treatment, cells were harvested and incubated with 1 mM protein cross-linker BMH for 30 min. The oligomerized BAX and BAK were detected by immunoblots using the corresponding antibodies. The nonspecific bands (22 kDa) served as the sample loading control.

Fig. 10. Down-regulation of BAX and BAK expression by siRNA attenuates erlotinib-induced apoptosis in H3255 cells. Cells with 75% confluence were transiently transfected with BAX and BAK siRNA or with non-specific siRNA, or with the same volume of medium as a nontransfection as described in Materials and Methods. Following transfection, cells were incubated in the presence of 0.1 μ M erlotinib (E) or the same volume of medium as a control (C). After 24 h of incubation, cells were taken from culture and cell pellets were divided into two aliquots. (A), One of cell aliquots was used for determination of BAX and BAK expression by immunoblots using anti-BAX and BAK antibodies. β -Actin was used as a loading control. (B), The other of cell aliquots was used for examination of apoptotic cells by counting the condensed and fragmented nuclei after staining with DAPI as described above. Data represent the mean \pm S.D. of three independent experiments, ** $p < 0.01$ compared with that in nontransfected cells, and * $p < 0.05$ vs. cells transfected with single siRNA.

Fig 1-1



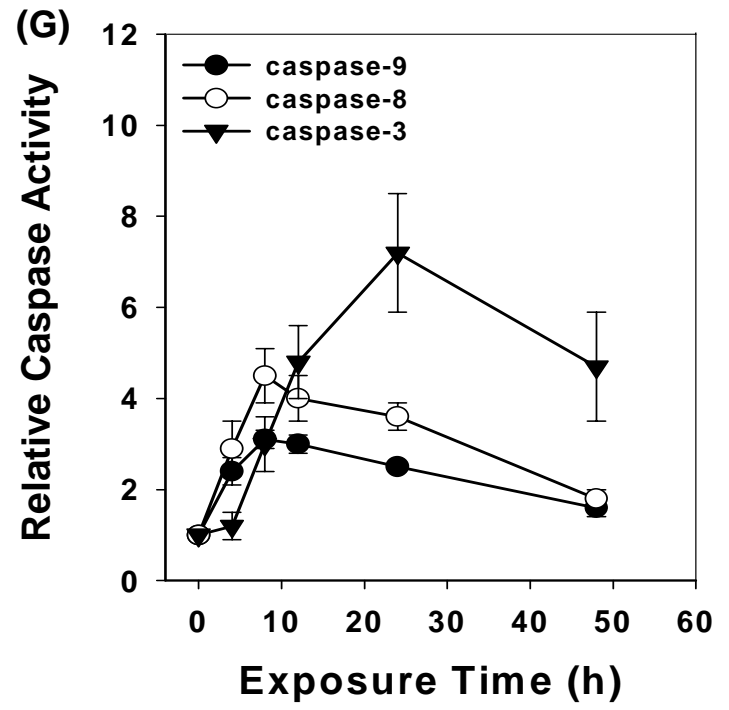
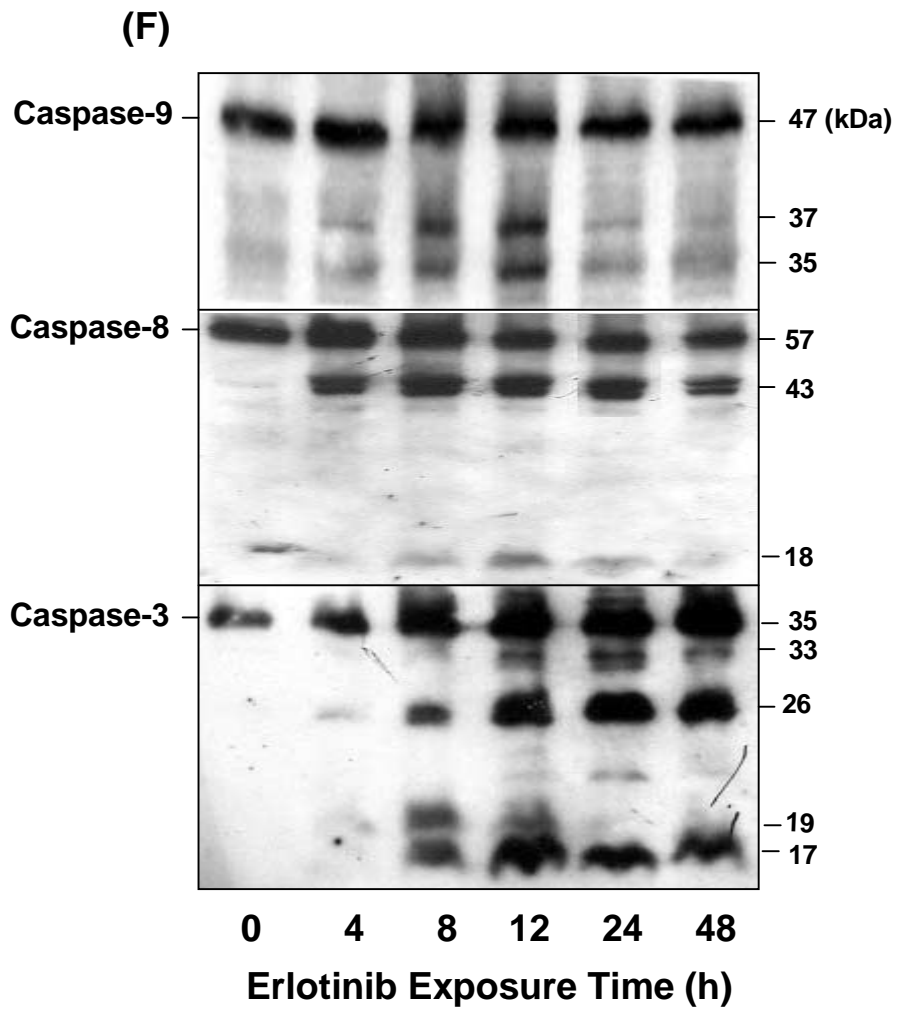


Fig. 1-2

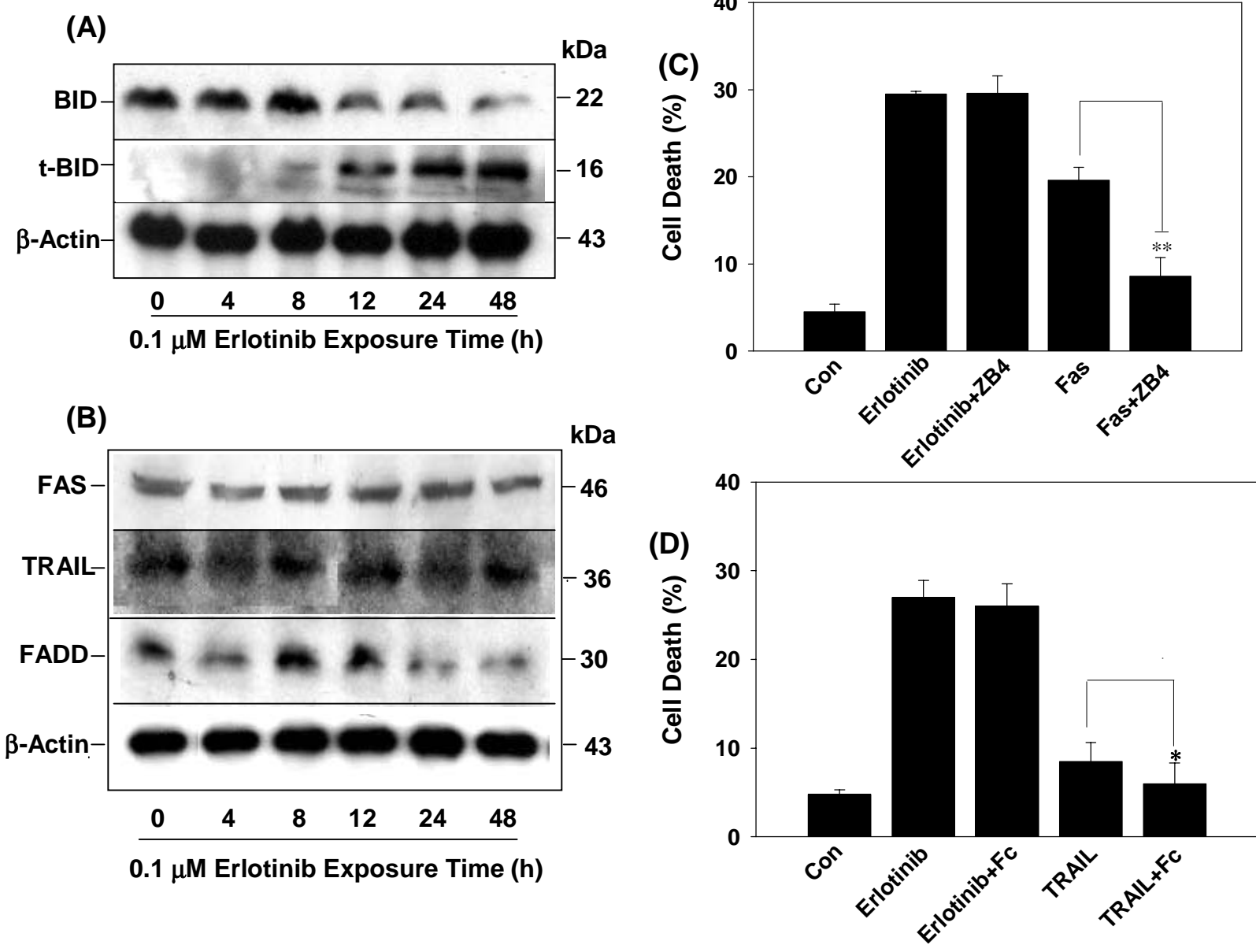


Fig 2

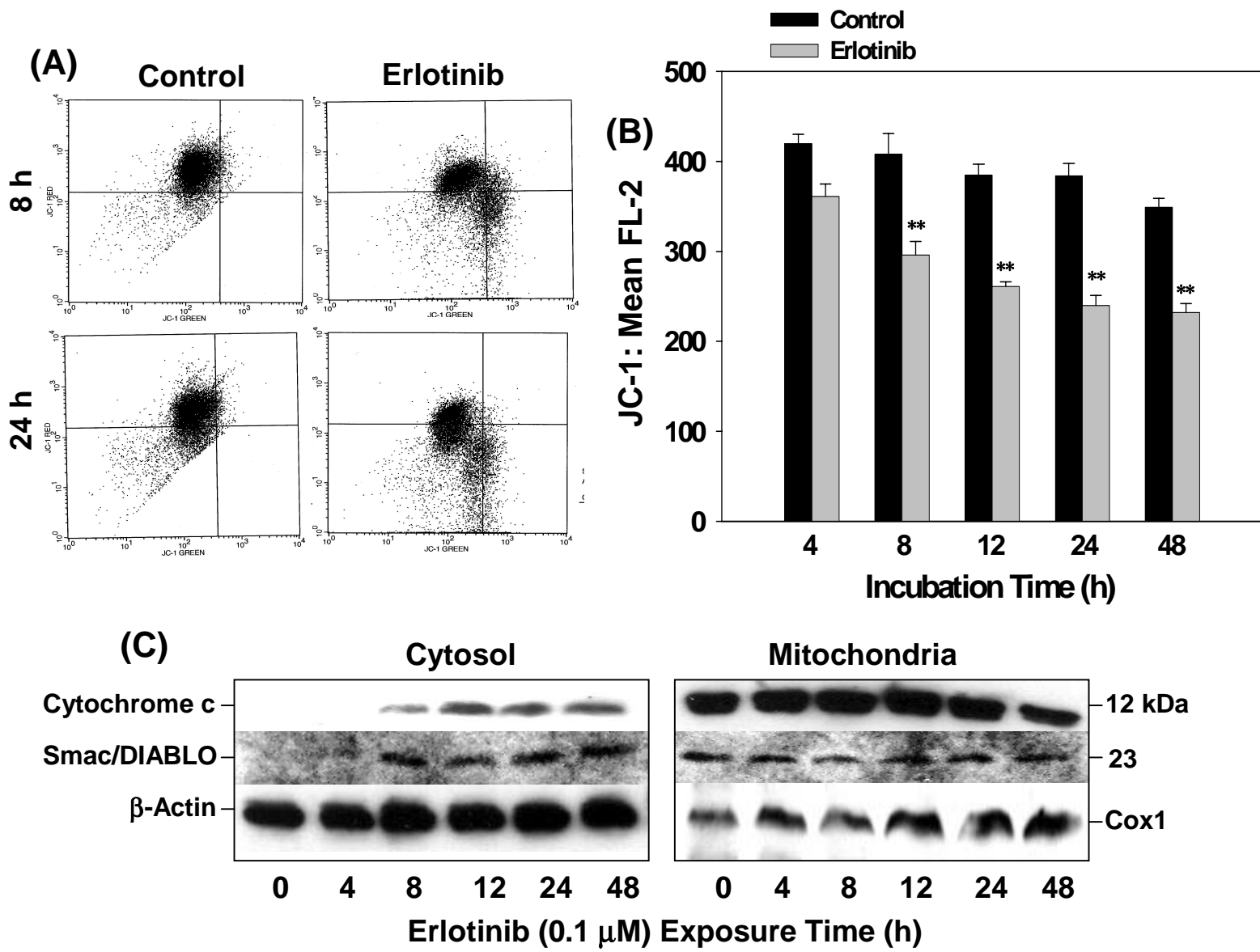


Fig. 3

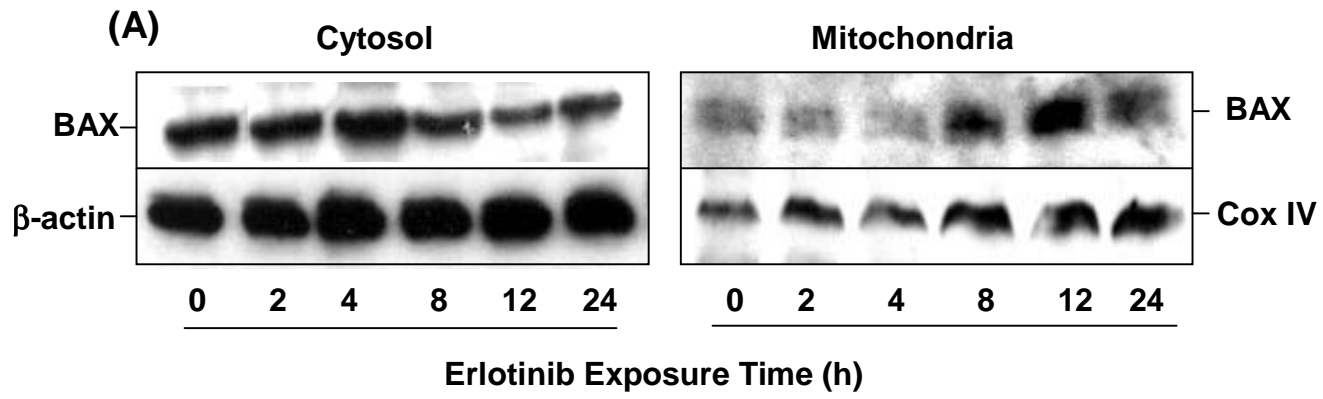


Fig. 4-1

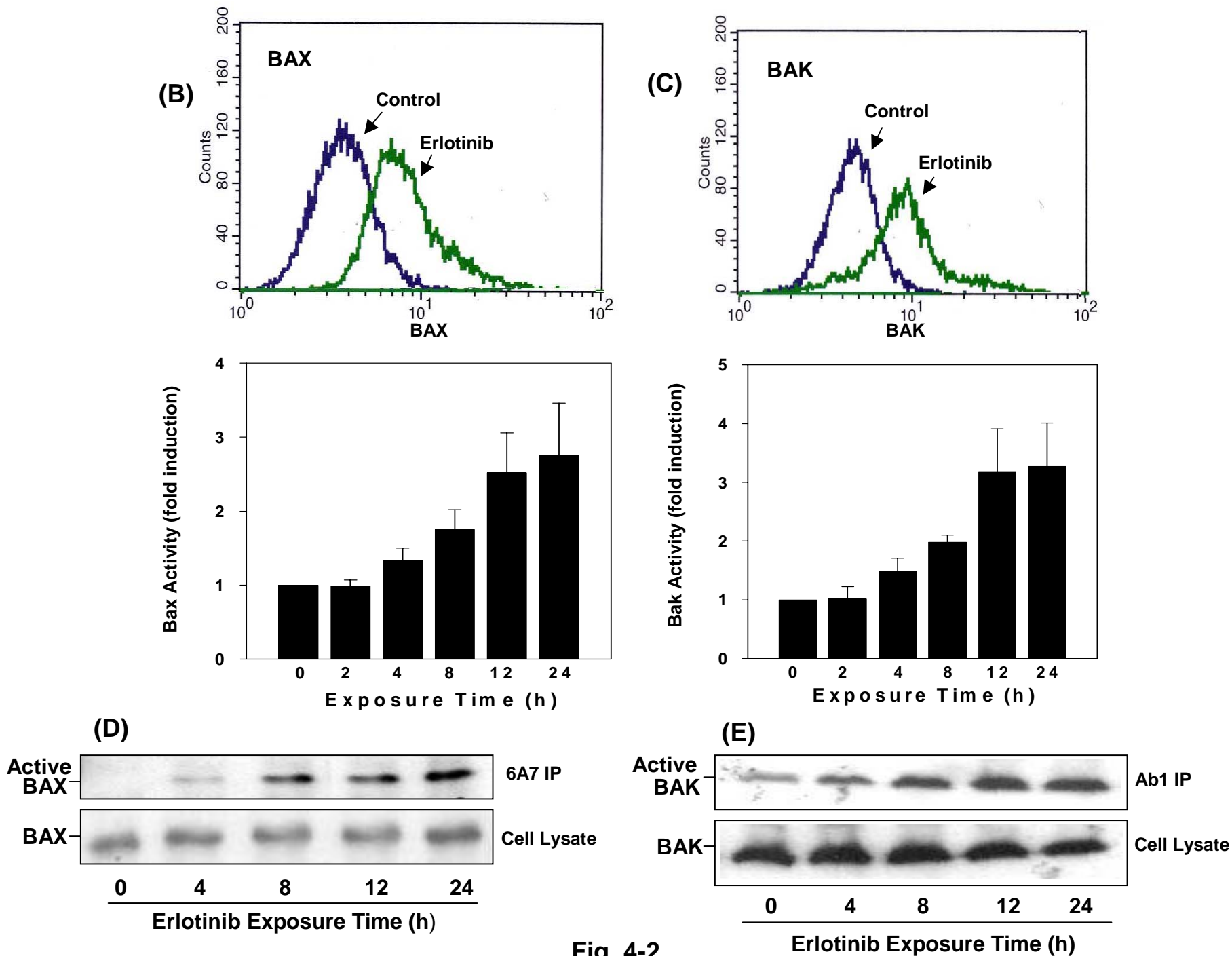


Fig. 4-2

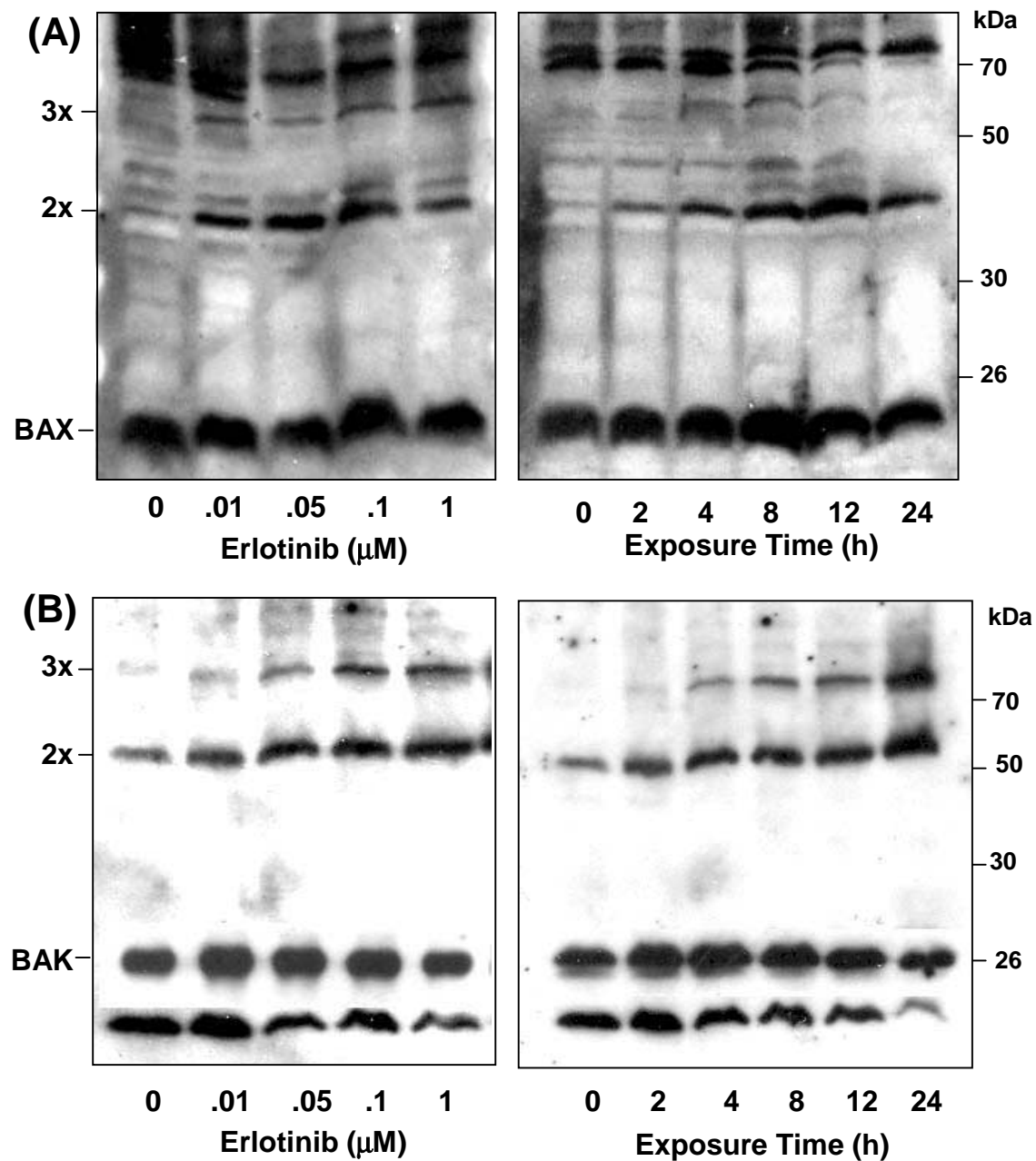


Fig. 5

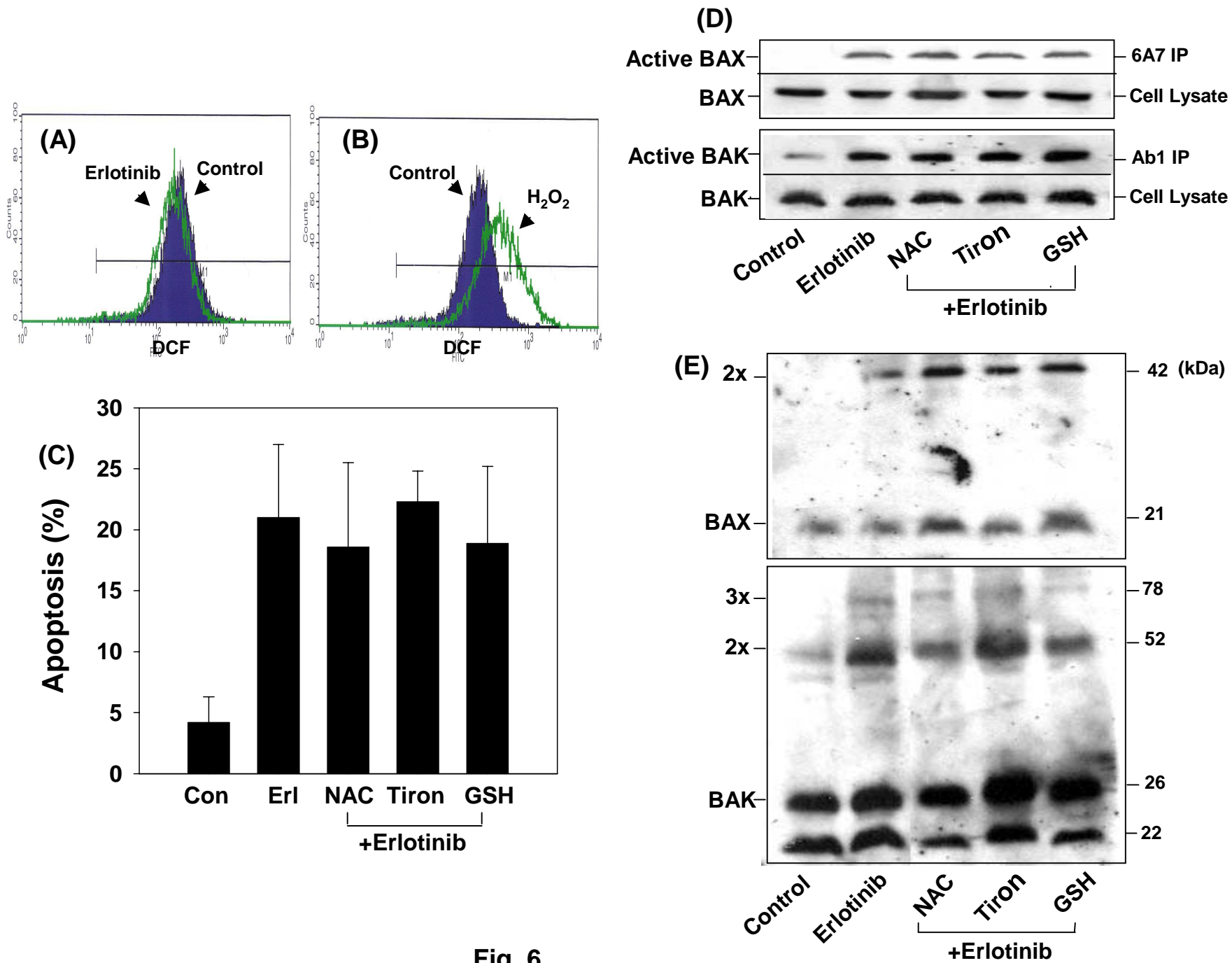


Fig. 6

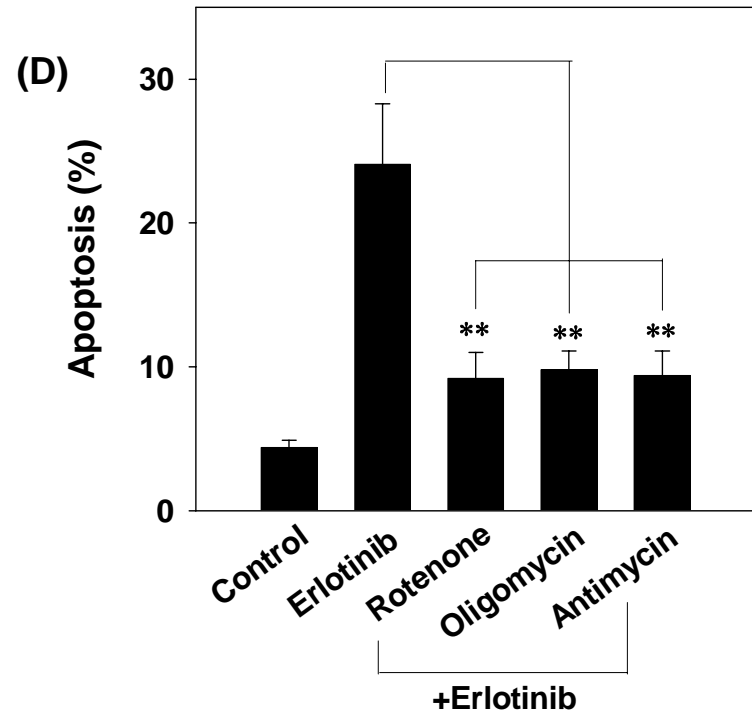
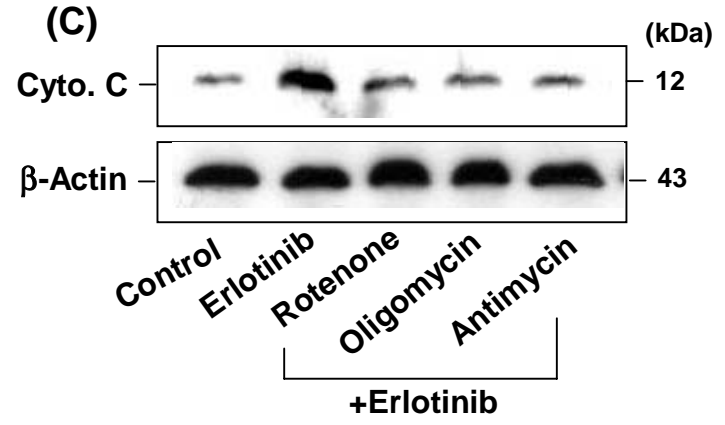
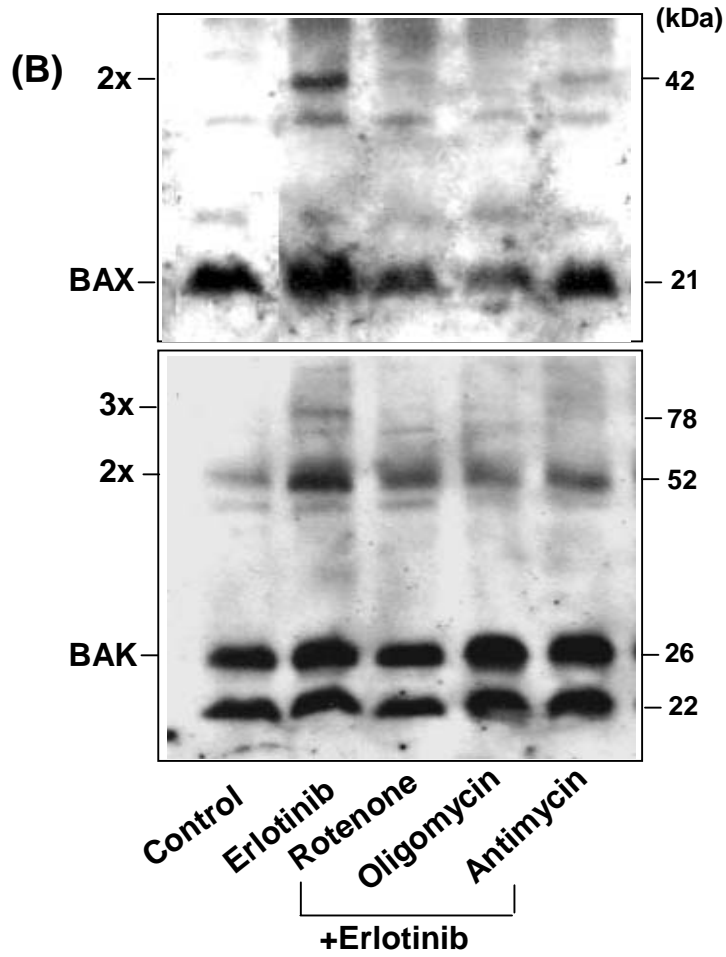
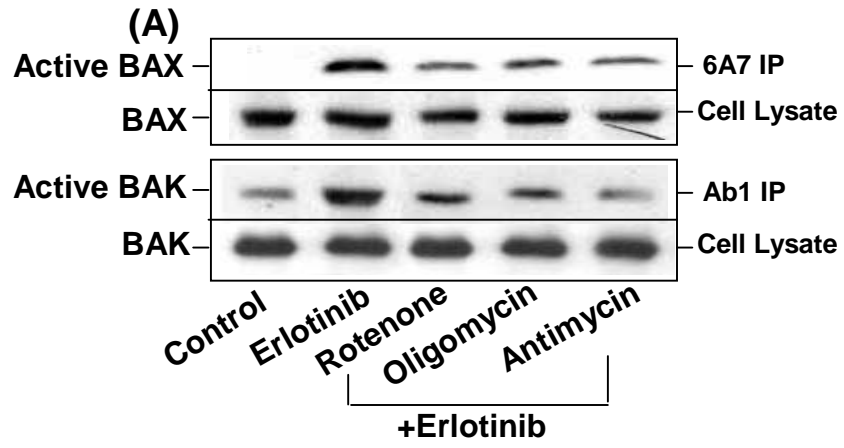


Fig. 7

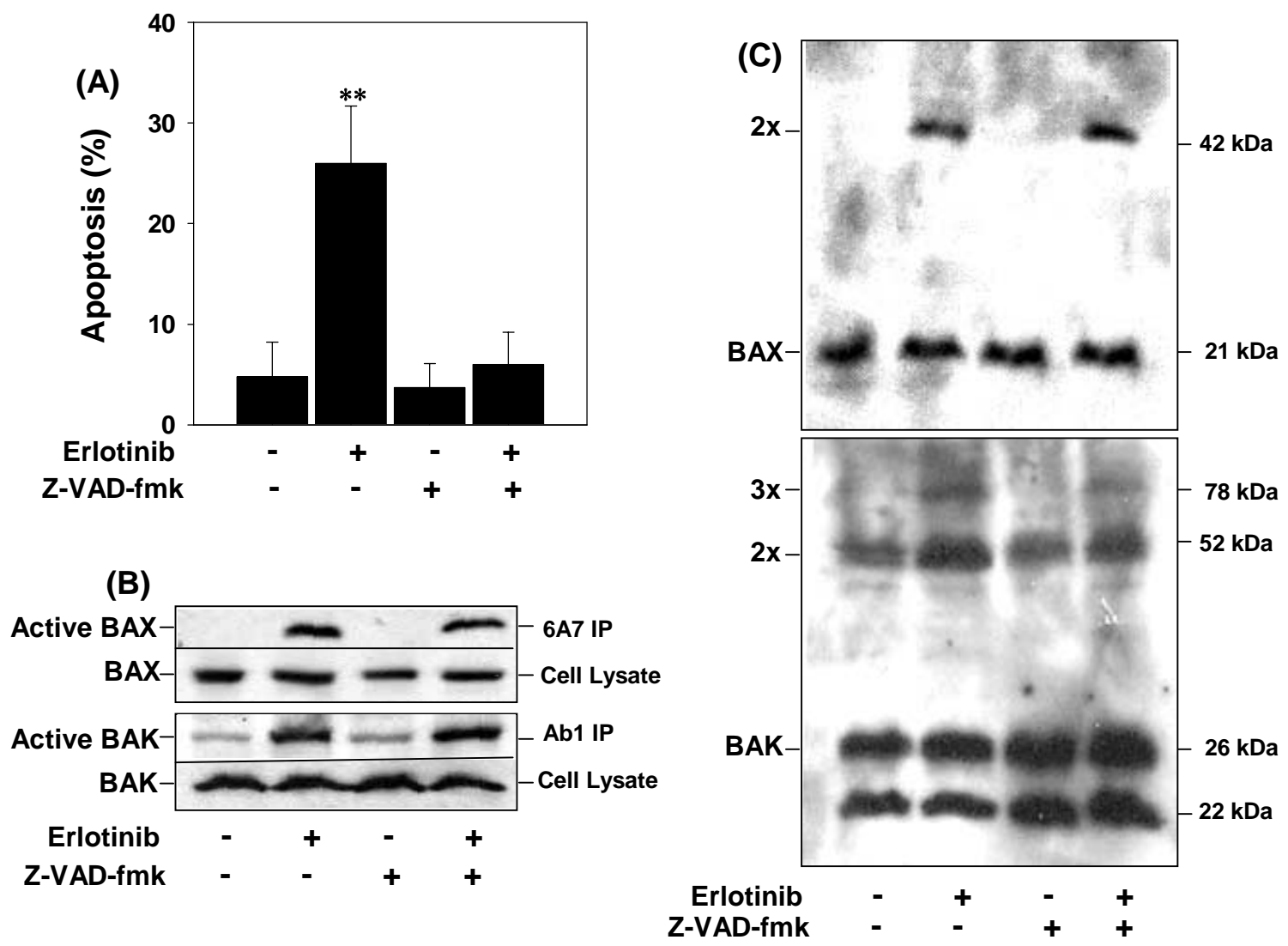


Fig. 8

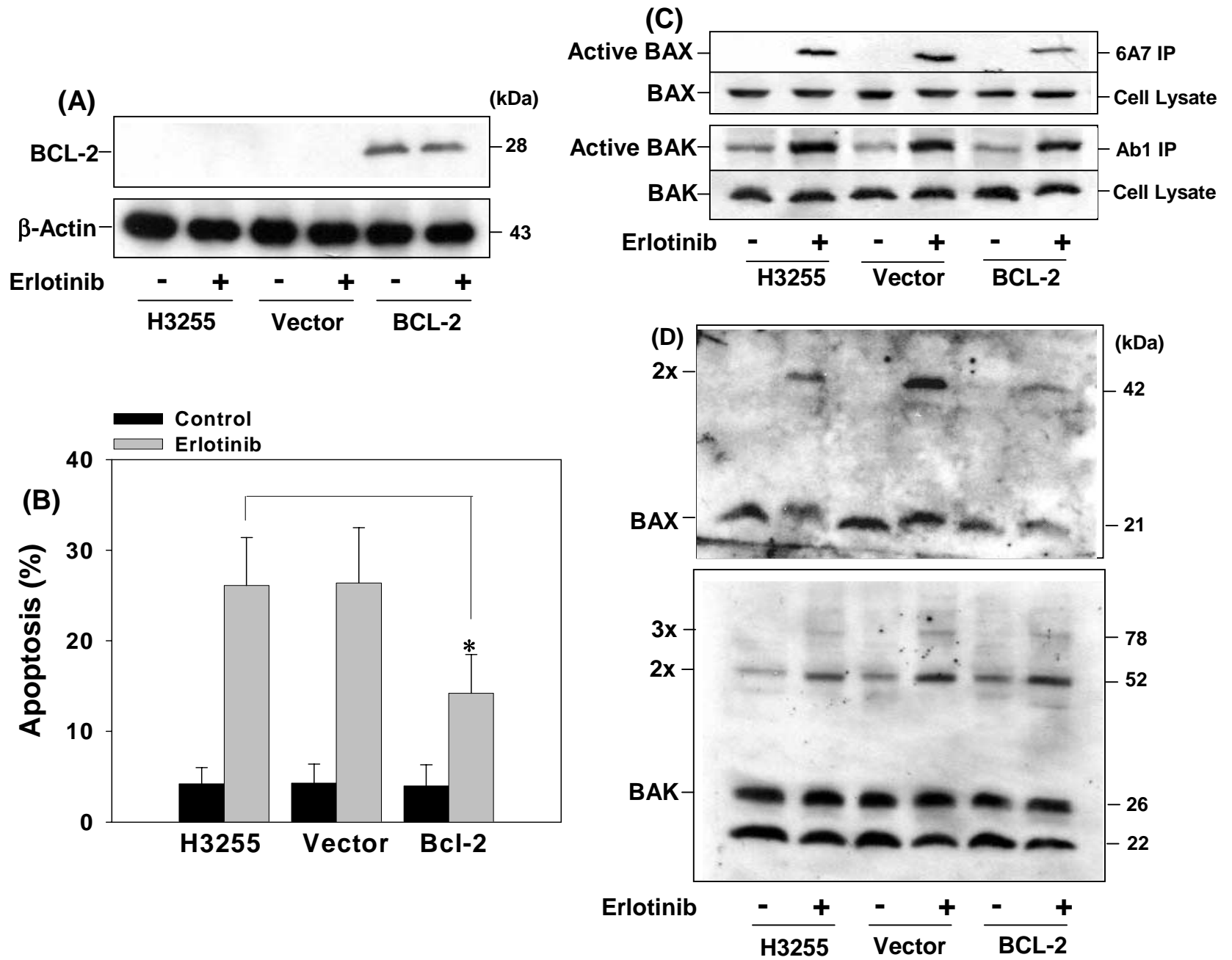


Fig. 9

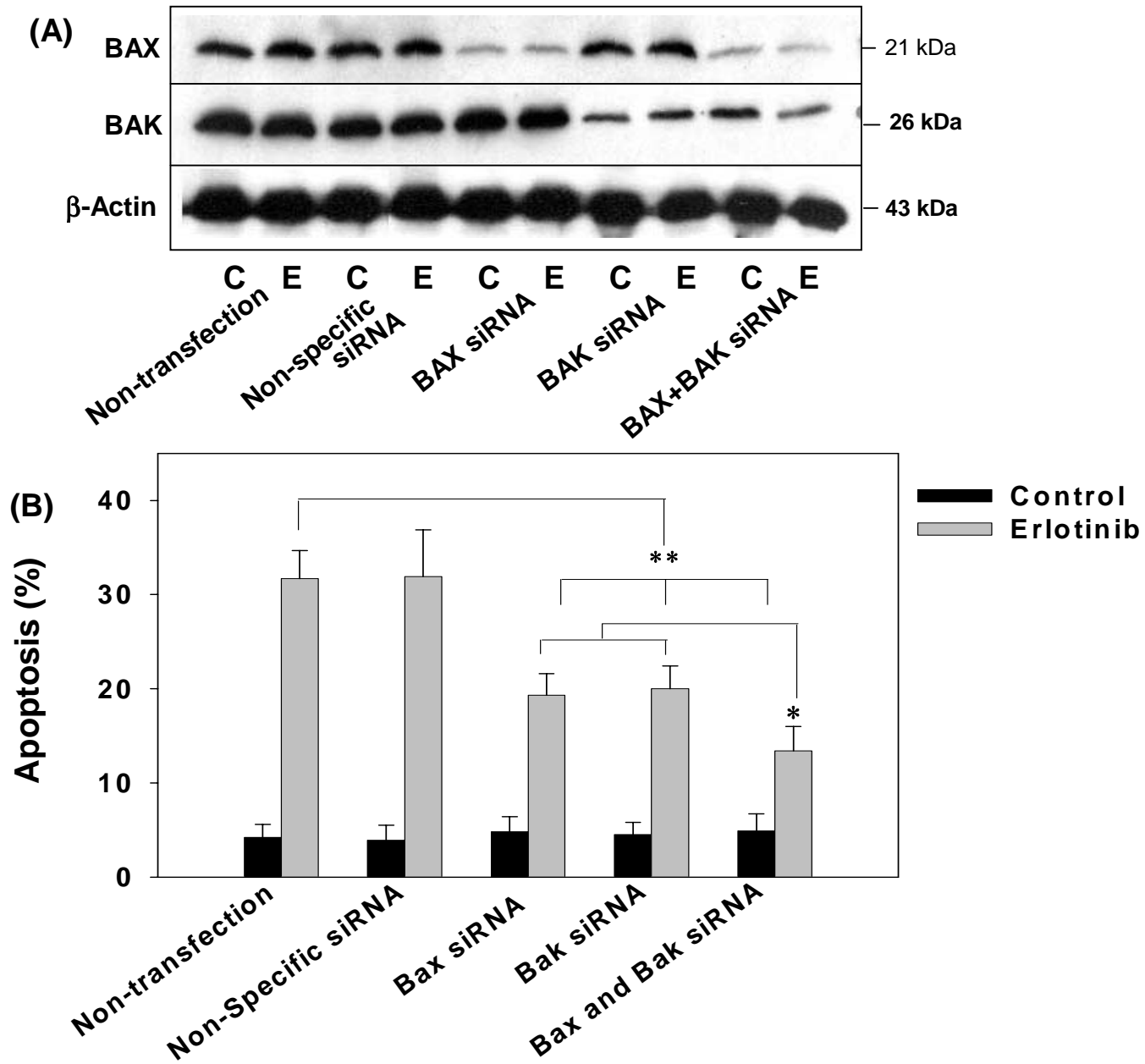


Fig. 10